UNIVERSITY OF CALIFORNIA
SANTA CRUZ

VIBRATIONS ANALYSIS OF DISCRETELY ASSEMBLED ULTRA-LIGHT AERO STRUCTURES

A thesis submitted in partial satisfaction
of the requirements for the degree of

MASTER OF SCIENCE

in

COMPUTER ENGINEERING

by

Anca - Mihaela Popescu

June 2019

The Thesis of Anca - Mihaela Popescu
is approved:

_____
Professor Mircea Teodorescu, Chair

_____
Professor Patrick Mantey

_____
Dr. Sean Swei

_____
Lori Kletzer
Vice Provost and Dean of Graduate Studies

Contents

List of Figures

List of Tables

Abstract

Vibrations of Discretely Assembled Ultra-Light Aero Structures

by

Anca - Mihaela Popescu

In this thesis, digital meta materials were investigated to prove this advancement in material science and manufacturability. The ultra light morphing wing having a twist design attests the cellular solids' versatility and scalability. The purpose of the research is to comprehend the impact of injected molded polymers and to implement analysis on the aero structure's behavior under vibrations.

This thesis presents a base-excitation modal testing technique for a lattice based aeroelastic wing by measuring the natural frequencies and the mode shapes of the lattice structure. The wing was vibrated through use of a shaker, which induced translational motion in the lateral direction of the wing. Two vibrometer lasers were used to detect the natural frequencies of the vibrations created by the shaker. The experimental results were compared with the finite element frequency simulations in Abaqus software, and the analytical model of a trapezoidal plate validated the results.

Acknowledgment

I would like to give special thanks to my reading committee, Professor Mircea Teodorescu, Professor Patrick Mantey and Dr. Sean Swei, for taking the time to read and comment on this thesis. Furthermore, I would like to thank my advisor, Mircea Teodorescu, for the support and for giving me the freedom to pursue my interest and to follow my own path.

I was honored to work on a project funded by NASA ARMD Convergent Aeronautics Solutions (CAS). Among the collaborators from NASA Ames, I need to thank individually Nick Cramer and Sean Swei for critical discussions and research assistance through the years. I would also like to thank the Center for Information Technology Research in the Interest of Society (CITRIS) for their support.

To my family, thank you for supporting me in all of my pursuits and for embracing my decision to move across the globe to follow my dreams. I am especially grateful to my parents, Gabriela and Adrian. I always knew that you believed in me and wanted the best for me. I must thank my cousin, Madalina, for always encouraging me and for the unselfish love and support given to me at all times.

1 Introduction

1.1 Motivation

Lattice-based structures enable many different configurations due to their ability to be disassembled into smaller elements and to be re-assembled, a feature that raises many unanswered questions that are my motivation for this thesis. This ability to reconfigure results from internal mechanisms that allow shape change and reorientation, such as morphing or folding, in this case a morphing wing structure. I was interested in analysing its mode shapes and in understanding its high stiffness to weight ratio, despite the difficulty in manufacturing.

Meta-materials with only a few types of components have advantages for building complex geometric structures of aircraft and space craft compared to the use of reconfigurable solids. The structural deformation and directional friction are highly linked, influencing the entire movement of the structure. Therefore, building aircraft wings from meta-materials is one efficient technique to provide versatility and scalability in digital systems. Being lightweight materials, the cellular solids bring improvements in relative stiffness and strength compared to relative density.

A digital cellular composite system in the shape of a morphing wing provides an exciting challenge in meta materials, and studying its behavior in vibration and analysing its natural frequencies aided in the understanding of their uniique characteristics. Having the same mechanical behaviors like elastomers, but with the advantage of a dramatically reduced mass, ultralight cellular materials stimulate the investigation combining material science, mechanics and aerospace.

1.2 Objectives of the present study

The objectives of this study and of this thesis:

- understanding the concept of one volumetric pixel, of an extended lattice structure and of the wing modular structure
- applying a base-excitation modal testing technique on one volumetric pixel, on an extended lattice structure and on the wing modular structure
- the analytical model of the wing modular lattice structure to validate the natural frequencies experimental results
- simulating and validating in Abaqus software the finite element frequency vibrations

2 Literature Review

2.1 Vibration analysis

Vibration analysis on different type of structures has a rich history in mechanics research. Determining the natural frequencies of rectangular plates has been investigated by several researchers in the past.

Lord Rayleigh has done a notable work bringing new information about the natural vibrations of completely fixed and completely free rectangular plates [32]. The natural vibration of a completely free plate was theoretically treated for the first time in 1909 by Ritz[34], proving the linear boundary value problems on the basis of variational calculus.

On the other side, a completely fixed plate also has been investigated by several authors which include Ritz . [34], Weinstein and Chien [41], Sato [22], Timotilta [37], Young [45], and others.

Plate vibration was investigated from early stages of vibration research [25]. Trapezoidal plates are often found on aircraft, missile and other structures. The natural frequencies and mode shapes were studied by Chopra and Durvasula for the simply supported trapezoidal plates, using the Galerkin method [11],[12]. The finite element method was the method to investigate free vibration of simply supported and clamped trapezoidal plates [30], while the method of time-averaged holographic interferometry was used by Maruyama et al [27]. The transverse vibration of a fully clamped trapezoidal cantilever plate of various thicknesses could be analysed by using energy techniques [23]. However, in the existing literature little research can be found in the literature for the analysis of vibrations in trapezoidal plates used in aircraft applications [7].

Weight reduction is one of the main factors in building aerospace systems, while still being able to transmit forces through space with the minimum possible weight and cost to the customer. Material properties influence the vibration

behavior of the application, however the material characteristics might be suitable for early-stage concepts, but not that suitable for the final application.
The natural frequencies of a simple basic undamped system vibrating is reduced to the mass m and spring of stiffness k, therefore the natural frequencies can be straight forward determined from:

$$f = \frac{1}{2\pi}\frac{k}{m}$$

Going to more complex geometries, like aerospace applications, the appropiate modeling through the estimation of the effective stiffness and mass enables calculating higher natural frequencies.

Reinforced fiber composites are hybrid materials, representing a combination of two or more materials, or of space and materials, which have attributes not offered by any one material alone. The hybrid materials provide the ability to synthesize and to design the properties of the material to its desired application. Cellular structures, as in our case lattice structures, are seen as hybrids of solid and gas, because the lattices have thermal conductivity and dieletric, due to the pores in the gas [4].

Vibration analysis proves the many additional benefits of the material selectioni from the high precision process of manufacturability. Digital meta materials become in this way a prompt method to achieve high performance in aerospace applications with critical dynamic modes, due to the performance metrics that scale with the square and the cube root of stiffness per mass density. The various geometries obtained from building blocks made of digital meta materials provide overall material life cycle, streamlining design and manufacturing, while founding competition with metallic and ceramic microlattices [17].

2.2 Digital cellular solids

Digital cellular solids represent meta-materials, constructed of a small number of physical building blocks. Meta-materials with a few types of component building-blocks can be used to build complex geometrical structures and high strength reconfigurable solids for applications in aircraft and space missions. [44].

Low-density materials are defined by stiffness, strength and spatial configuration of voids and solid, which creates cellular architecture and solid constituent properties. The mechanical efficiency is improved by controlling the dimensions and periodicity of the architecture, enabling a self supporting cellular material with a lower order of magnitude of the density[36].

Cellular materials with low weight and superior mechanical properties are inspired by natural materials, honeycomb or foamlike structures, such as wood, cork, plant parenchyma, sponge or trabeculer bone. Micro and nano scale building blocks with an ordered hierarchy improve mechanical properties of the metallic microlattices [47].

Solid and hollow-tube ceramic octet-truss lattices behave different in compression due to the local buckling induced by the high aspect ratio of the strut length to nanoscale wall thickness, in contrast to nanoscale TiN trusses or ceramic composite. These materials have aspect ratios low enough to allow the nanoscale strengthening effect of the wall thickness to dominate. Therefore, digital cellular solids are lightweight materials with improvements in relative stiffness and strength compared to relative density [10].

The systems made out of digital materials is different of analog fabrication systems, because it proposes a method for fabrication from discrete parts with discrete relative local positioning. These type of systems could have various architecture, due to their versatility.

One of the motivation for the architecture is the biological analogy, that brings self-assembling and self-reconfigurable capabilities with both extrinsically functional products and intrinsically functional machinery while being made of the same fundamental set of units.

Digital materials employ a finite number of types of simple discrete components which could create large structures respecting the local-only rules, achieving trivial adaptation to various shapes at large scale.

Lattice-based structures could provide different configurations due to their ability to be disassembled into smaller elements and to be re-assembled. This ability to reconfigure results from internal mechanisms that allow shape change and reorientation, such as morphing or folding. However, the strain of the compliant material changing shape limits the degree of reconfiguration [21].

Lattice-based structures are structures also found in nature where there is a high stiffness to weight an advantageous ratio, such as bone or wood. This advantageous ratio is achieved through the geometric configuration and sparse distribution of material, that could be reproduced in man-made materials, such as engineered foams. There is a difficulty in manufacturing these complex geometries with traditional processes, but additive manufacturing such as projection micro-stereolithography represents the solution to create millimeter-scale bending and stretch dominated lattice structures with polymers, metals, and ceramics.

Struts and nodes are the primary components of the digital material construction system, which are assembled to make voxels, which create the lattice structures. The purpose of the nodes is to capture and orient the struts properly so it can achieve an octahedrON. Voxel to voxel orientation is considered by proper alignment and orientation.

A digital cellular composite system in the shape of a morphing wing, has a manufacturing process that enables mass production by using high-performance composites. The elements of the digital cellular composite elements are assem-

bled by hand with reversible mechanical connections [20].

Ultralight cellular have the same mechanical behaviors like elastomers, but with the advantage of a dramatically reduced mass. The new approach is represented by soft robotic structures made out of digital cellular materiials, replacing the high mass density of elastomers difficult to use for high-performance aeronautics structures.

Meta-materials could be created by these discrete lattice parts, having properties determined by their base material and lattice geometry. Varying their geometry, it is possible to attain continuum robotic behavior across a range of moduli with the same set of parts. In this way, it is possible to build lightweight, integrative and deformable structures.

The assembled blocks are made of unidirectional fiber composite beams and looped fiber load-bearing holes being reversibly linked, like chains, to form volume filling lattice structures. These parts are mass produced and assembled to fill arbitrary structural shapes. The resolution is prescribed by the part scale, which is chosen to match the variability of the boundary stress encountered in an application. Each identical part represents a cellular material, making an assembly that has a predictable behavior [9].

The nonlinear elastic behavior of the multi-axial elastic instability of the lattice is caused by the elastic buckling of the strut members. The geometry is similar to a Jahn-Teller distortion of an octahedral complex taking into consideration the orientation about the octahedral centers. The antisymmetric twisting stress response in 2D lattices is caused by elastic folding or pleating across a lattice structure, while the plastic deformations are present as well.

Lattice materials are a class of cellular materials with a regular and periodic microstructure. These materials combine properties that cannot be achieved by uniform fully solid materials, such as lightness, stiffness, strength and high energy absorbing capabilities [40].

Digital cellular solids pursue the existing work of cellular solids by decomposing the periodic lattices which compose these solids into discrete parts which can then be mass-manufactured. If there is a reversible connection, the digital cellular solids could be reconfigured and repaired to adapt to changing mission criteria [6]. The current approach has been demonstrated in aerospace applications such as shape-morphing aircraft or reconfigurable, mesoscale structures.

The digital cellular solids confer as well improved performance over conventionally manufactured rigid pressure vessels. Examination of toroidal pressure vessels shows that the digital cellular solids compete with other proposed habitat construction designs, maintaining the core capabilities.

An ultralight aero structure with high stiffness-to-density ratio is built from digital composite materials, providing the wing the capability to shape according to the flight conditions [14].

The conventional FEM approach for modeling a high-dimensional lattice is challenging, due to the difficulty to analyze and visualize the integrated large-dimension lattice structure in real time. The new technique is an efficient and effective modeling approach that is both suitable for structural analysis and control design.

Generating and propagating higher harmonics in lattice structures creates dispersion, nonlinearity and modal complexity, resulting in an augmentation of the functionality landscape of the lattice and making the nonlinearly generated wave features display modal and directional characteristics that are complementary to those exhibited by the fundamental harmonic [16].

Lattice structures have a dispersive and asymmetric wave propagation. These structures absorb the energy, due to their superior strength at low density. The resilience of lattice structures is caused by extremely large deformations and their asymmetric nature [33].

Lattice structures present defects in the form of perturbations to the units'

mass, inter-element force and on-site potential generated by the bi-stable elements. Nonlinear dynamics are introduced in the structure by repelling magnets through the inter-element force. The structures defects are overcome with propagating waves by varying parameters of the lattice [18].

Different lattice architectures, rectangular, sheared and hexagonal, create dispersion surfaces that overlap in frequency and beaming direction, proving frequency dependent directional energy flow [46].

However, the system stability could be lost because of the vibration of beams, since nonlinear vibrations could occur under external forces that will influence the normal behavior, leading to damage in the system structure [1].

2.3 Aircraft wings

There are different techniques proposed involving dynamic measurements such as modal analysis, acoustic emission, and ultrasonics. There is a necessity in studying and performing an experimental modal analysis for a wing of an aircraft model [15]. There are two techniques for minimizing the structural vibrations:

- passive control, which add damping to the structure, but it reduces its vibration
- active control, which involves control forces generated by an external energy source and applied through actuators. The active systems could bring a strong control and could be designed to influence a number of vibration modes

Mechanical vibrations are abundant and ubiquitous in environment, providing no limitations in their applications. These vibrations are using electrostatic devices, electromagnetic field and utilizing piezoelectric materials.

Different beam shapes ranging from rectangular beams to triangular beams in terms of resonant frequency, output voltage and efficiency proved that the

shape can have a great effect on the output voltage and therefore maximum output power density. The deformation, strain and voltage of a triangular vibration energy harvester is more than those of a rectangular or trapezoidal one.

Jet flux or turbulent fluid flow create high-intensity acoustic loading in high-speed aircraft panels. The high-intensity noise created is combined with high temperatures, because of the aerodynamic heating and jet exhaust impingement. Also, in high-speed military aircraft, the issue of acoustic fatigue becomes relevant, due to broadband random noise and high-level harmonic tones [28].

A simplified model of the complex structural models used in high-speed aircraft components is the isotropic beam. The multi-modal beam response is considered for the finite element modal approach.

The mode shapes of the linear system are used to output the static finite element cases into modal coordinates. The nonlinear stiffness coefficients are extracted from the regression analysis, having a model with direct non-linear and non-linear cross-coupling terms. Free vibration behavior of quasi isotropic carbon fiber laminated composite plates are numerically, analytically, and experimentally investigated [2].

Applications that involve unwanted structural vibrations, such as automotive, marine, civil and medial fields use fiber reinforced polymer composite materials, due to high strength-to weight and stiffness-to-weight ratios. These polymers provide excellent chemical and corrosion resistance.

The control and suppression of unwanted structural vibrations can be achieved with piezoelectric smart structures, where structural dynamics and control theory are taken into consideration for the design. The smart piezoelectric structures represent a structure with sensors and actuators coordinated by a controller and based on piezo actuators. The smart structure has the ability to adapt to changes in the environment and to perform self-diagnosis [42].

2.4 Laser vibrometer

The natural frequencies and mode shapes of aircraft structures are measured using base-excitation modal testing technique. A shaker is often set onto the base or one of the edges of the structure, inducing a lateral translational motion. The displacement of the shaker base and the painted spots of the wing are measured by photonic probes. The frequency response functions are calculated with a spectrum analyzer.

There are different ways to measure dynamic parameters of the tiny read/write head suspension:

- fixed suspension and excited it by a mechanical shaker; a small force transducer is used to measure the force applied by the shaker, and a photonic probe is used to measure the response.
- the excitation device is a suspension's servo actuator and a white noise current in the servo actuator as the force portion of the frequency response function
- an electromagnetic actuator focused on a small ferromagnetic target glued onto the test structure. These electromagnetic exciters are designed to provide a force which approximates a point load.
- a pulse air to induce free vibration of a head-suspension assembly, and used a laser Doppler vibrometer to measure its response.

The hammer impacts induce time domain response of fiber-optic sensors, which are transformed into frequency domain. The natural frequencies and amplitudes are the first displacement and strain mode shapes, based on the frequency transfer function. The use of impact hammers or shakers as exciting sources and bonded accelerometers as sensing elements represents the conventional modal analysis approach, which ensures resolution and sensitivity.

However, large structures with a special geometry require high complexity. The detection of vibration parameters in practical composite structures is implemented based on embedded fiber-optic sensors with fiber Bragg gratings (FBGs). In this case, a signal proportional to the second time derivative of the displacement is considered.

There are a few FBGs techniques:

- irradiating the fiber with a UV beam filtered with a suitable silica phase mask reproducing the grating structure
- the lateral illumination of the optic fiber with two intersecting coherent UV laser beams (interferometric writing)
- punctual variation of the refractive index of the fiber (point to point writing).

Multi-reference sine sweep tests are performed that combines the speed of multiple-reference random testing with the force levels of sine sweep tests, by sweeping simultaneously independent source signals at different individual frequencies [29].

Sinusoidal sweep methods allow for higher RMS input loads, lead to much cleaner FRF and provide symmetric and antisymmetric excitations to emphasize symmetric and antisymmetric modes. The disadvantage of sinusoidal sweep methods is that the method is single-reference and must be run in series, which extends overall testing time. If there are two shakers mounted on wingtips and two shakers mounted on the horizontal stabilizers, then a total of four sine sweeps would need to be performed: wing symmetric, wing antisymmetric, horizontal stabilizer symmetric, and horizontal stabilizer antisymmetric. In order to perform multiple sine sweeps in series is to combine the individual different frequencies to sweep at the same time, a technique will be called a “multi-sine sweep’. All

sine sweep phase combinations are supposed to be performed at the same time to generate multi-reference frequency response functions.

Multi-sine excitation is a multiple-reference excitation technique with the superior signal-to-noise ratio of traditional single-reference sine sweep excitation. Several sweeps simultaneously over the desired frequency range of interest are performed, but each excites the aircraft at a different frequency at each instant in time. So, all sine sweeps can be performed at the same time.

In aircraft applications, the most common experiments are made of four electrodynamic shakers used to excite each wing tip and each horizontal stabilizer tip. Descriptions of the different shaker excitation methods which are representative of those used in aircraft ground vibration testing are described below:

- Conventional Sine Sweep Tests. Four separate wing symmetric, wing antisymmetric, horizontal tail symmetric, and horizontal tail antisymmetric sweeps from 50 to 1 Hz. Since there is only one independent source signal per sweep, only one of the load cells can be used as a reference signal for calculating FRF's

- Conventional Burst Random Test. All four shakers excited simultaneously with independent burst random input signals. All four shaker load cells are used as FRF references

- Multi-Sine Case: Symmetric, then Antisymmetric Ratio Sweep

Two thin faces of metal sheet bonded to a visco-elastic core made a constrained-layer damping sandwich structure, which provides an efficient way to suppress noise and vibrations in the structure which is thin and light. This type of constrained-layer damping structures are useful for automotive, aerospace and naval applications.

Good signal-to-noise ratio is obtained in the following methods of excitation:

- shakers inject high energy levels, giving vibrations over the noise floor. Mounting a shaker requires skilled experiments
- hammer excitations are dificult to repeat at the same physical location of the structure, creating the DOF-jitter

The wavenumbers were estimated through three methods using the function of frequency:

- the spatial Fourier method, which suffers of a limited wavenumber domain resolution
- the Prony approach and the wave fitting approach, which both have a a good wavenumber domain resolution. Their estimations are comparable with the analytical results, proving the estimated equivalent Young's modulus function of frequency. Moreover, the wave number could be estimated through the wave fitting approach.

Multi-dimensional vibrometry at high speeds cannot be performed by multi-dimensional vibrometry, because it relies on single-point measurements and on beam scanning, which results in utility and precision limitations. This issue is solved by creating a laser vibrometer that performs high-speed multi-dimensional imaging-based vibration and velocity measurements with nanometer-scale axial resolution without the need for beam scanning[26].

Several industrial applications require high-speed vibrometry, like nondestructive inspection and diagnosis of aircraft components, microelectromechanical systems (MEMS), automotive brakes, musical instruments, hard disk drives.

The laser Doppler vibrometry is a convetional method for laser vibrometry which is unable to perform vibration measurements at high speed. The Doppler vibrometry is based on single-point measurements and relies on beam scanning.

The ultralight micro lattices fracture after contact with loading platens, because of the reduction in stiffness, which makes the measurement of the compressive stiffness of these ultralight lattices with conventional contact techniques a major challenge. Non-contact resonant approaches are used for modulus measurements in solid materials, at both small and large scales. The Laser Doppler Vibrometry is coupled with Finite Elements Analysis for the reliable extraction of the Young's modulus in ultralight microlattices[35].

The effective Young's modulus of the sample in the direction normal to the face sheets can be obtained from the detection of resonant frequencies by close-form analytical solutions or fitting to Finite Element models.

However, contact measurement techniques are not applicable to Young's modulus measurements on ultralight cellular materials with deformation created by fracture events, because the necessary load application results in the characterization of a post-fractured lattice.

Therefore, the scanning laser Doppler vibrometer system is used to obtain the mode shapes of a vibrating structure surface. The modal properties, natural frequencies, mode shapes and modal damping ratios show changes of physical properties of a structure, like the mass, stiffness and damping[43].

With modal properties, the damage of the vibrated structure could be detected, located and characterized, since the laser Doppler vibrometer offers accurate, non-contact surface vibration measurement. The vibrometer is based on Doppler shifts between the incident light from and scattered light to the system.

Cellular materials, such as polymers, metallic, ceramic or hybrid, provide mechanical proficiency due to architectural optimization and base material selection. The base material is deposited in form of films with a thickness lower than microns, establishing mechanical size effects at nanoscale[39].

3 Discretely Assembled Ultra-Light Structures

When mass strongly influences performance and cost, the desired materials are strong and stiff ultra-light materials for structural applications. In aerospace, specific mechanical properties lead the design of aerospace structures with critical dynamic modes. [4].

Starting from one volumetric pixel and implementing the building block approach, it was proven that ideal stiffness and strength behavior can be achieved at ultra-light mass density, using industrial mass production processes. Therefore, an ultralight, reversibly assembled lattice material composed of injection molded thermoplastic building blocks displays stiffness and strength [17].

3.1 One Volumetric Pixel

The digital material concept uses a single three dimensional geometric shape as a basis for the cellular solid construction. In this project the used voxel was a cubic octahedron shown in figure 1. Cuboctahedral lattices were assembled from injection molded octahedral unit cells named voxels.

One voxel has a pitch, or unit cell length, of 3 inches, and quadrilateral strut cross section to enable injection molding, with a cross-sectional area of 2.63 e10-3 square inches, as it is represented in figure 2.

3.2 Extended Lattice Structure

A system made of digital materials consists of modular building blocks forming larger structures of arbitrary size and shape, where struts and nodes are the primary components of the digital material construction system, which are assembled to make voxels, which create the lattice structures [21]. Voxel to voxel assembling creates different configurations by proper alignment and orientation, where the strain of the compliant material changing shape limits the degree of

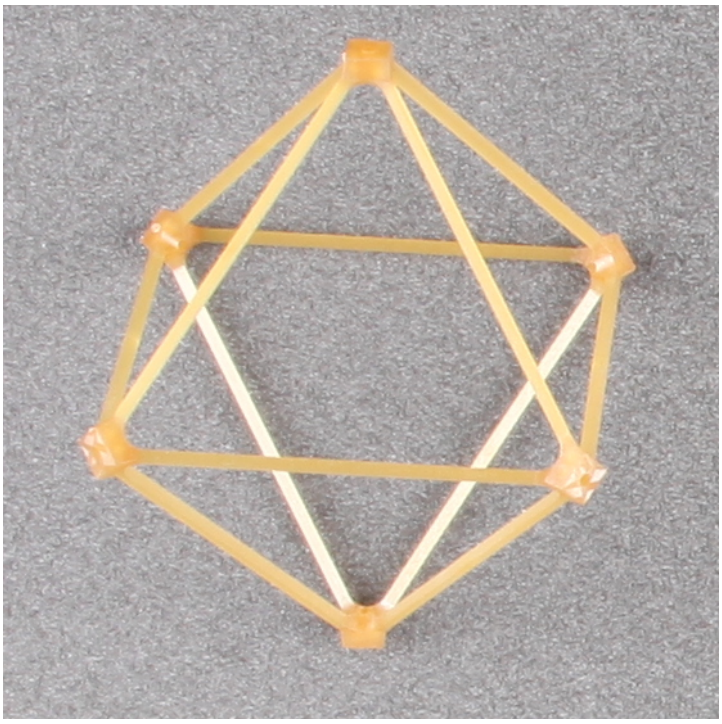

Figure 1: Cubic octahedron volumetric pixel

reconfiguration.

By using building block based assembly as an intermediate and temporary approach to our aircraft wing application, it represents a method that helps understand the material lifecycle, potentially streamlining design, analysis, manufacturing, and servicing to fully realize by proving therefore the potential of lattice materials in transformative structural applications [17].

In the intermediate experiment, the lattice structure is built of 2 by 2 by 4 voxels (figure 3), which will be simulated and tested in order to get the validation of the method applied in this study.

3.3 Aircraft Wing Lattice Structure

From one single volumetric pixel to an extended voxels substructure to an aircraft lattice structure, there is only a matter of building process. The aircraft wing is made of cuboctahedral voxels with a 3 in pitch and kite shaped strut

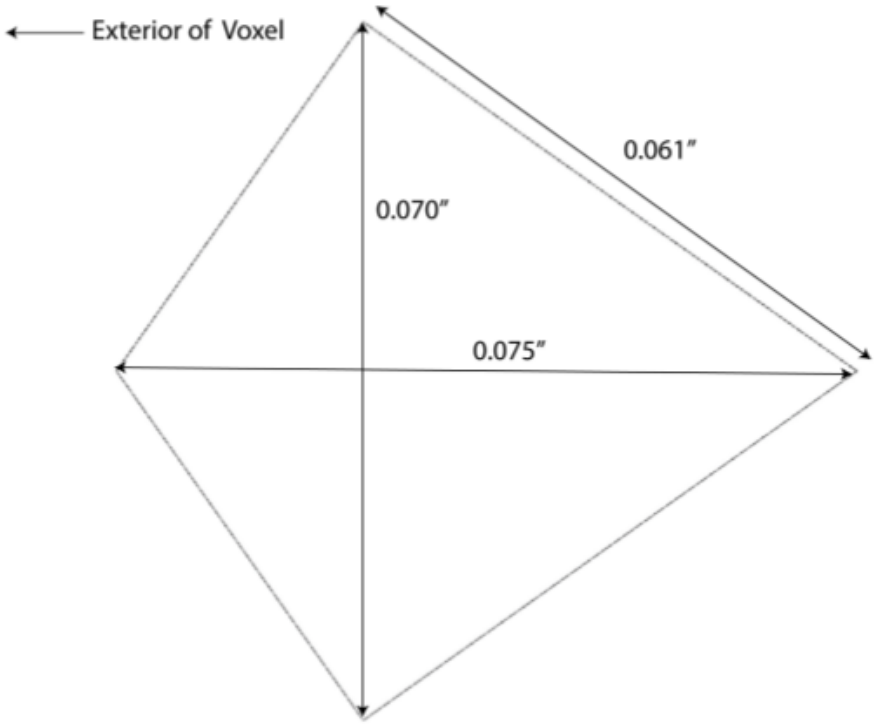

Figure 2: Cross section geometry of the injection molded struts

cross-section, as presented in figure 2, injected molded with Ultem 2200.

The designed digital material wing has a 13.5 foot wing span with a 45^o sweep and a total of 2061 voxels. The wing substructure was designed using the previously presented voxels as the fundamental components, and it is represented in figure 4:

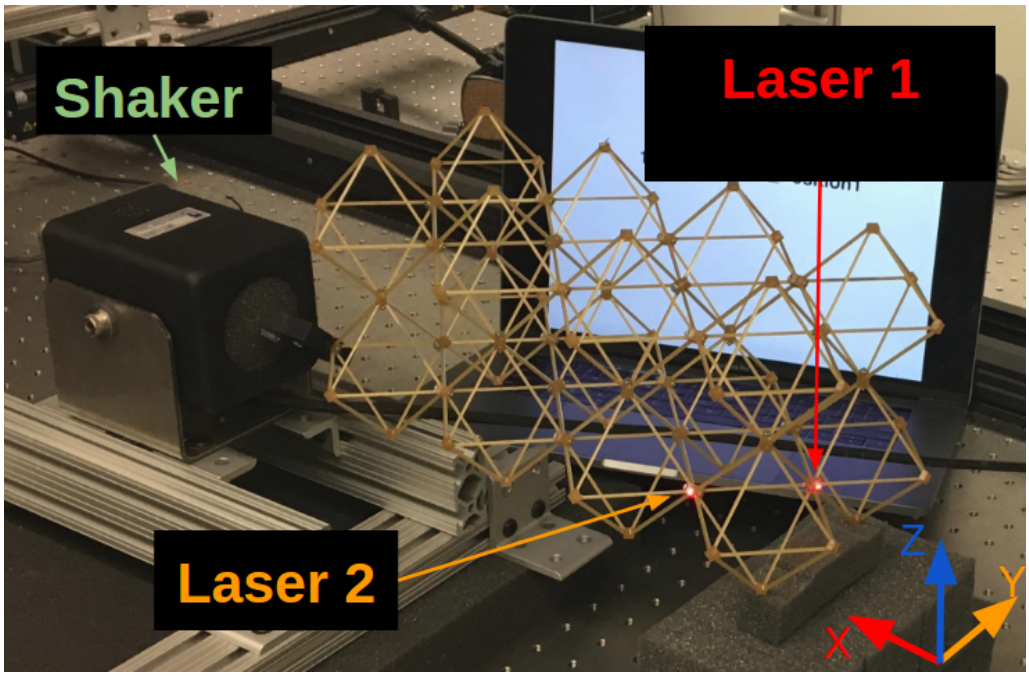

Figure 3: Extended Lattice Structure

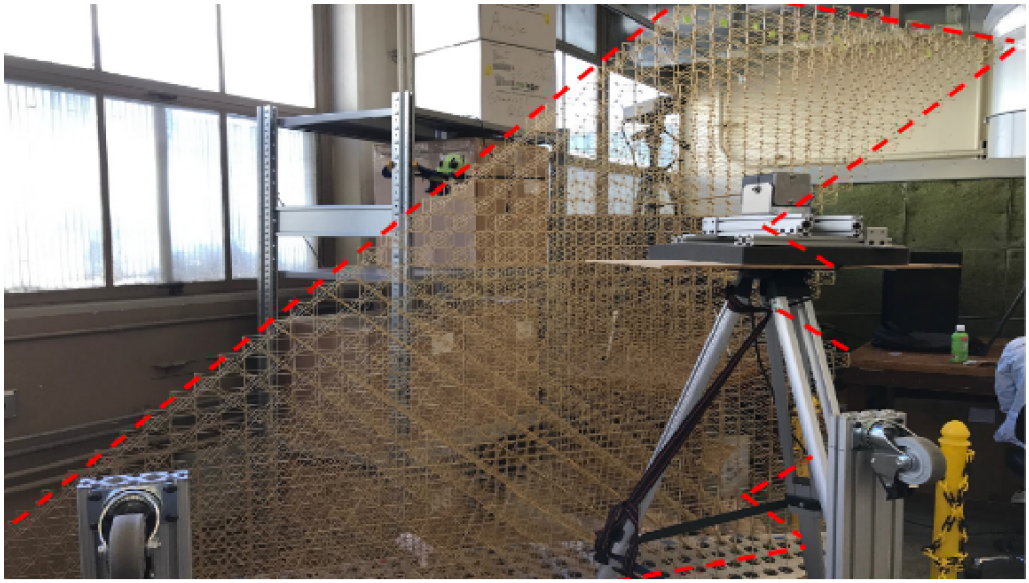

Figure 4: Aircraft Voxel Wing

4 Vibration Analysis and Validation

4.1 Experimental Analysis

4.1.1 Basics of vibrations

Vibration analysis on different type of structures was always an interest in the research field. The best way to approach our application is to understand the vibrations from the fundamental part of volumetric pixels, which is a beam extracted from a volumetric pixel.

The natural frequency of the beam can be computed using the the following fundamental formula of vibration:

$$f = \frac{3.5156}{2\pi L^2}\sqrt{\frac{EI}{\delta A}} \tag{1}$$

where L is the length of the beam, δ is the density of the beam, E represents the stress applied to it, A is the area of the cross section. The value of E is $6.89 \times 10^9 N/m^2$ and the value of I is $0.25 \times 10^-12m^4$. The density of the beam is $1411.6kg/m^3$.

We know that the length is $L = 42E^{-3}m$, with an area of $A = 2\times\frac{1.8mm1.9mm/2}{2} = 1.71E^{-6}m$.

Also, the modulus of elasticity is $E = 6.89E^9N/m^2$ and $I = 0.25E^{-12}m^4$.

The length of the beam in our experiment is 0.042m, while the area of the cross section is 1.71 mm^2. By calculating the natural frequency the result is 269.86 Hz.

$$f = \frac{3.5156}{2\pi L^2}\sqrt{\frac{EI}{\delta A}} = 269.86Hz \tag{2}$$

In order to validate the analytical result, the detached beam was tested with the vibrometer laser. The oscillation of the beam was captured by a high speed

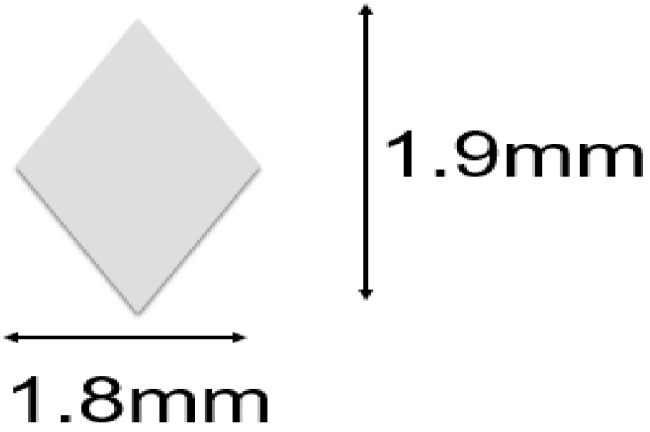

camera, Fastec il5, with a frame rate of 2,270 fps, with an average period of oscillation of 8.5 frames, which is approximate 3.5 ms (fig. 5). The beam was

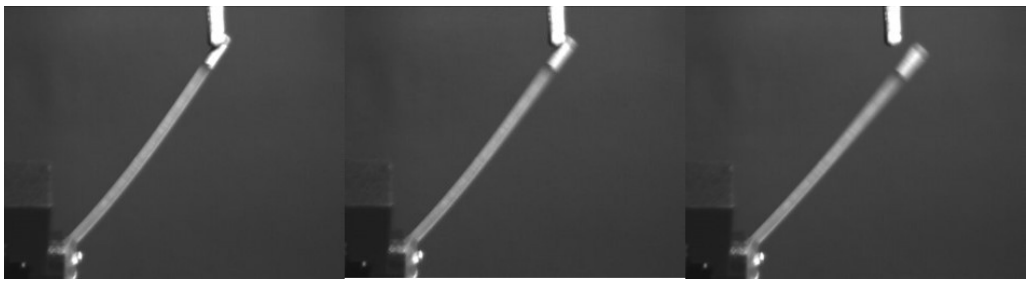

(a) t = 0 (b) t = 1*10E-6 (c) t = 2*10E-6

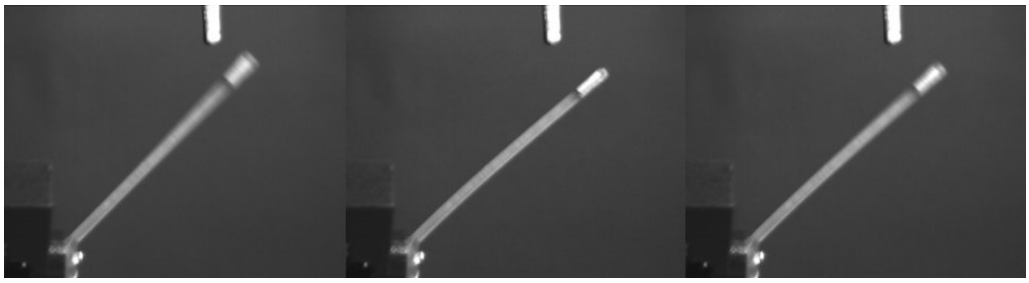

(d) t = 3*10E-6 (e) t = 4*10E-6 (f) t = 5*10E-6

Figure 5: High Speed Camera

excited by the shaker, while the laser was pointing on the beam (fig. 6). The laser technique involves sine testing, i.e. testing of a structure which is assumed to be effectively linear, excited by a sinusoidal input excitation.

The fundamental bending frequency, the first bending mode, detected was 270 Hz, while the second and third mode of vibration were captured as well in

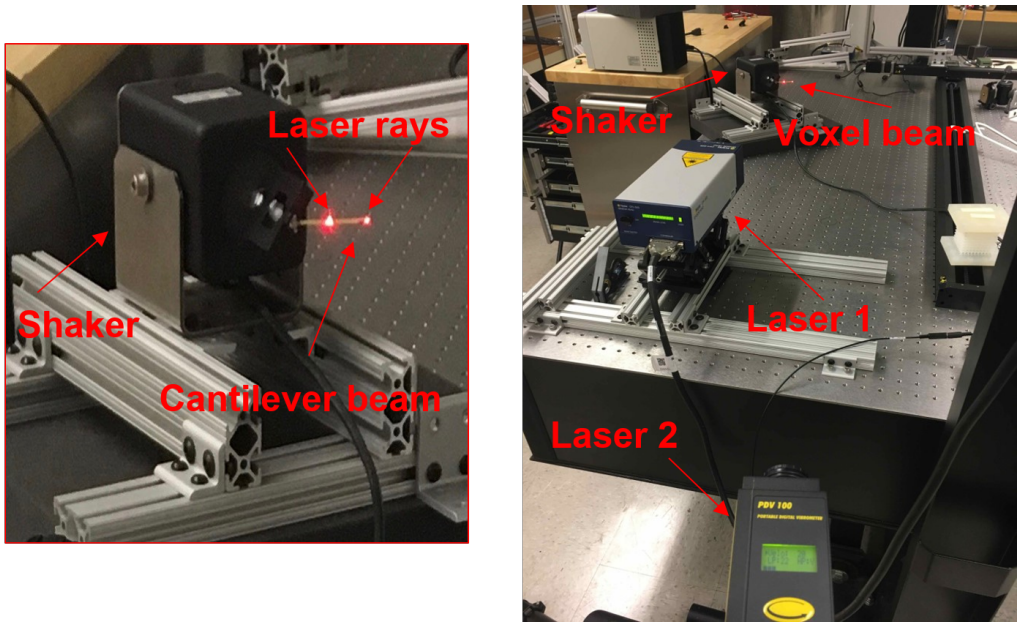

Figure 6: Laser Setup

the same experiment (figure 7). It has be proven the laser vibrometer measurement technique is a valid method for the natural frequencies detection in our application.

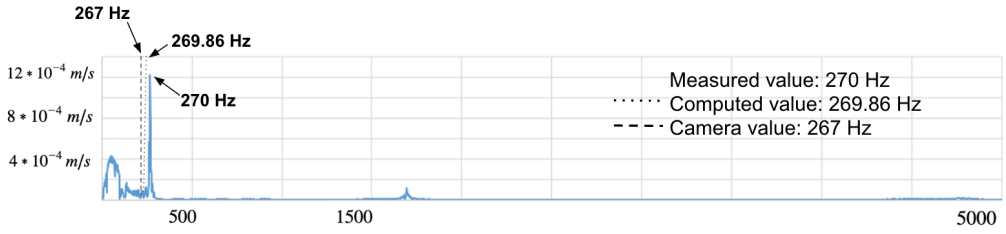

Figure 7: Beam Bending Modes

4.1.2 1 volumetric pixel

In the experimental testing, the mechanical excitation of one voxel was created by the shaker mounted in one of the corners of the volumetric pixel. The laser vibrometer pointed on different spots on the voxel and from different directions: we tested the voxel on 2 different pitches and on the beam as well (fig. 8 and fig. 9).

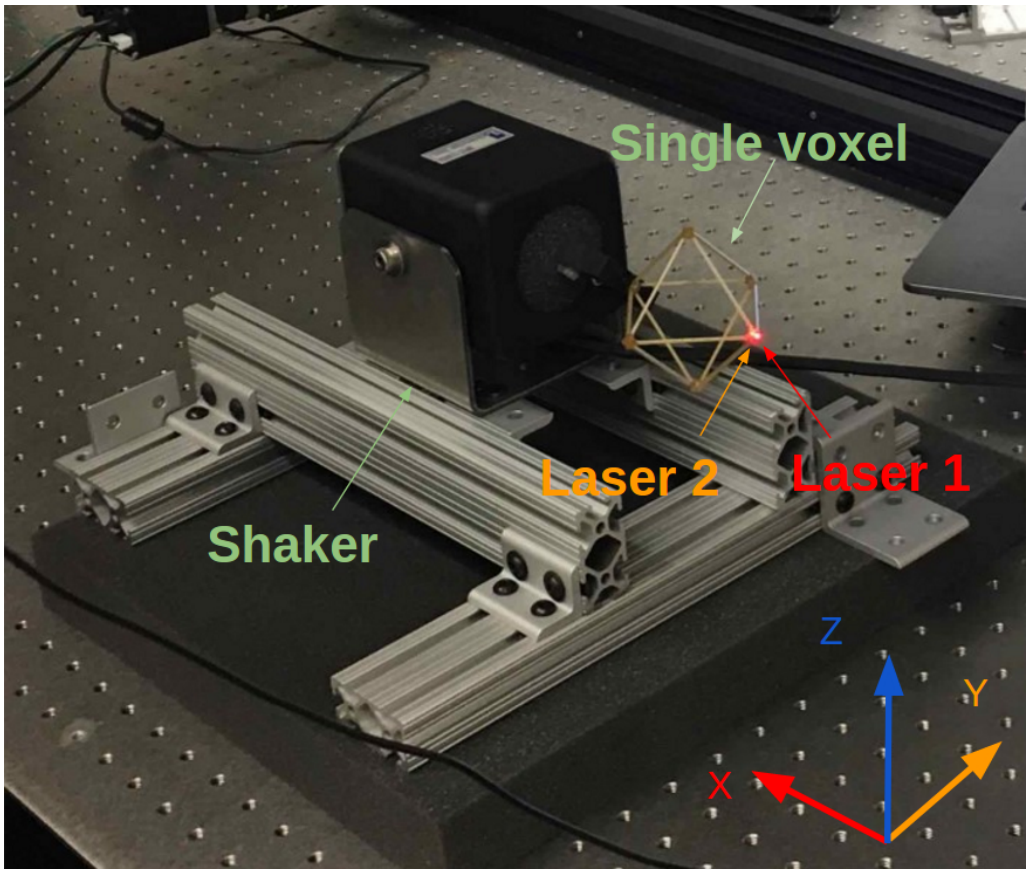

Figure 8: Voxel Experimental Setup - Pitch Measurement

The laser results showed different frequencies due to the fact the vibrations were measured from different locations and angles, even if the shaker excitations were the same (fig. 10). From the first plot, we can see the natural frequencies were more significant from the second laser direction. On the second plot the frequencies shown are the frequencies at the same values from the other side of the pitch and from the beam of the voxel, but with 3D Finite Element Frequency

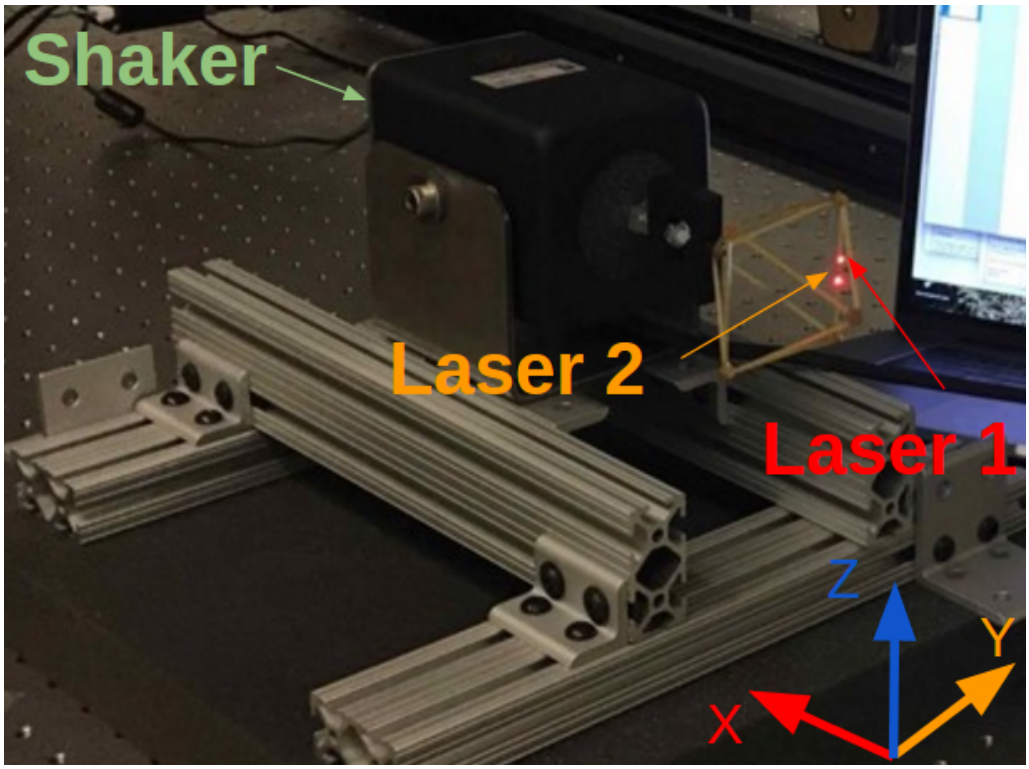

Figure 9: Voxel Experimental Setup - Beam Measurement

Simulation a much lower amplitude.

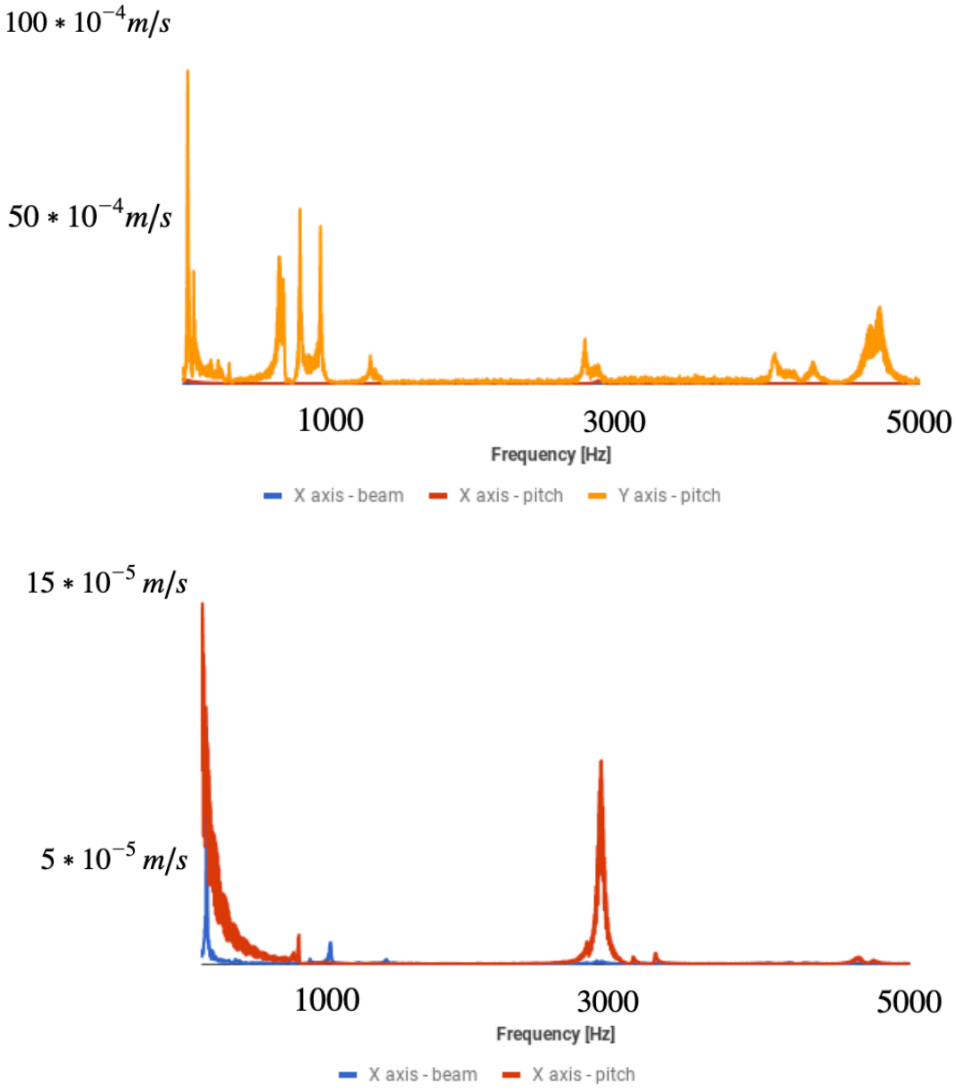

Figure 10: Natural Frequenices of 1 Voxel

4.1.3 Extended lattice structure

The vibrometer laser experiment is reapplied in the same setup, as shown in the following figure:

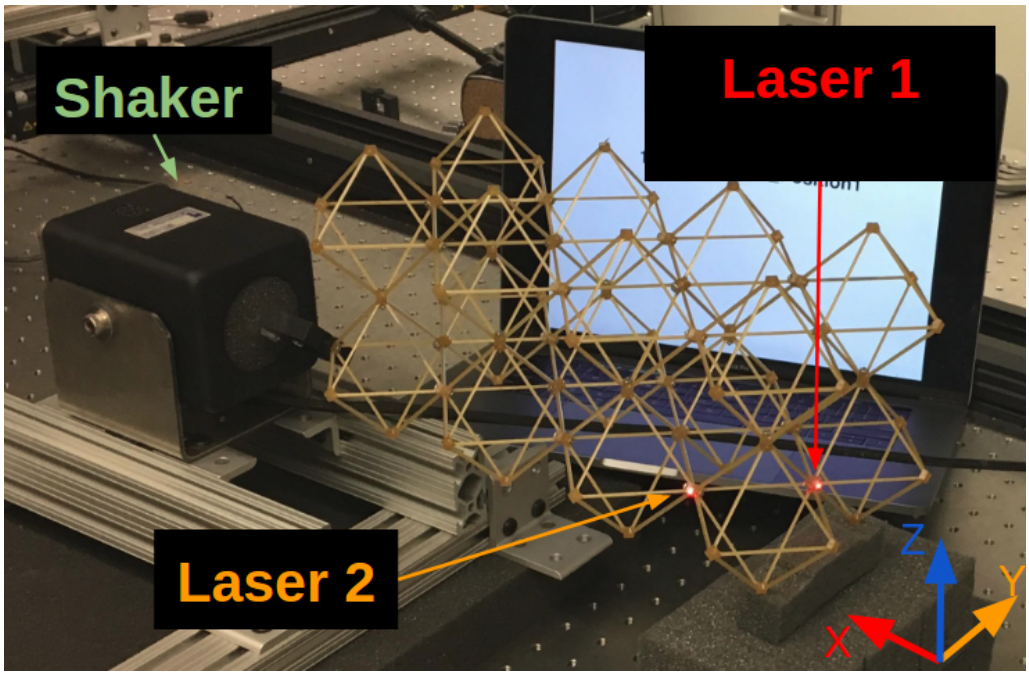

Figure 11: Extended lattice structure tested

The bending modes were caught between 100 and 600 Hz (fig. 12). After 1000 Hz, the extended lattice structure does show any mode of vibration caught by the laser.

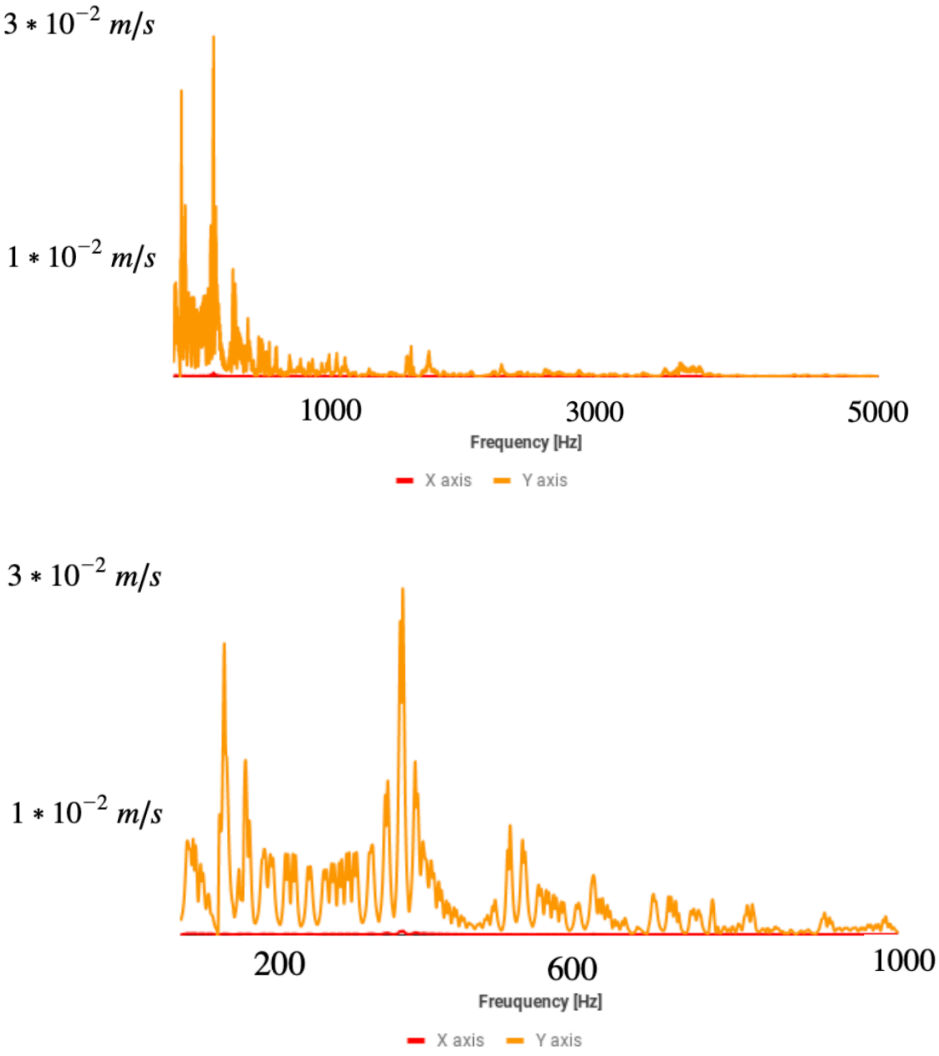

Figure 12: Natural frequencies of the extended lattice structure

4.1.4 Aircraft lattice wing experiment

In the experimental testing, the mechanical excitation of the wing was created by the shaker mounted in the lateral part of the structure (fig. 13).

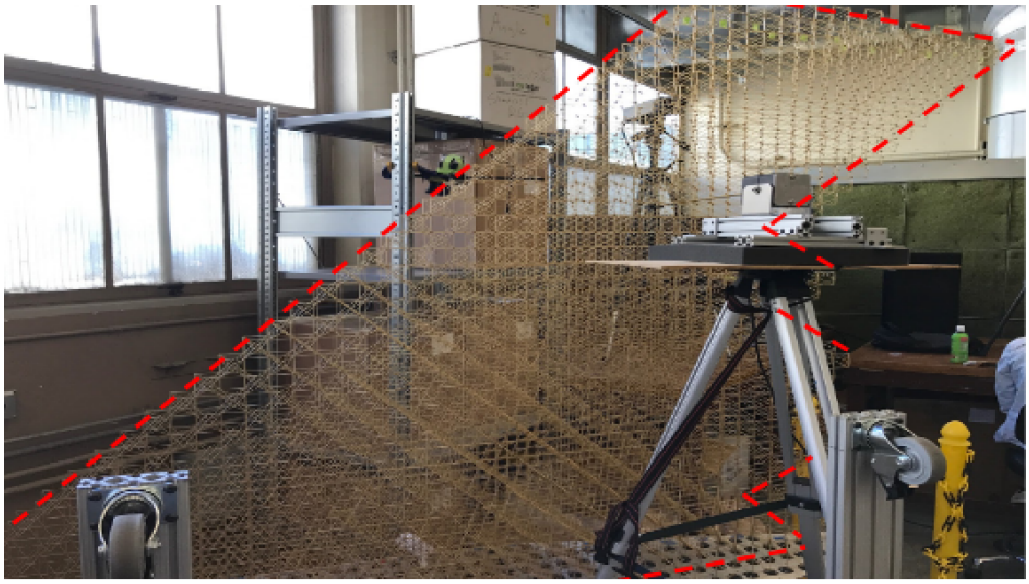

Figure 13: Wing Structure - Shaker Excitation Experiment

The excitation was a repetitive sine wave applied in the middle upper part of the wing. Two vibrometer lasers were mounted to measure the vibrations of the excitation. The upper edge of the wing has 12 modular lattice structures, so we had 12 measuring points, which were tracked from different direction in order to catch the vibration from different axis (fig. 14).

The two lasers were oriented from different directions, as shown in figure 15, representing X and Y axis. The natural frequencies detected from the lasers measurements will be presented in the next section.

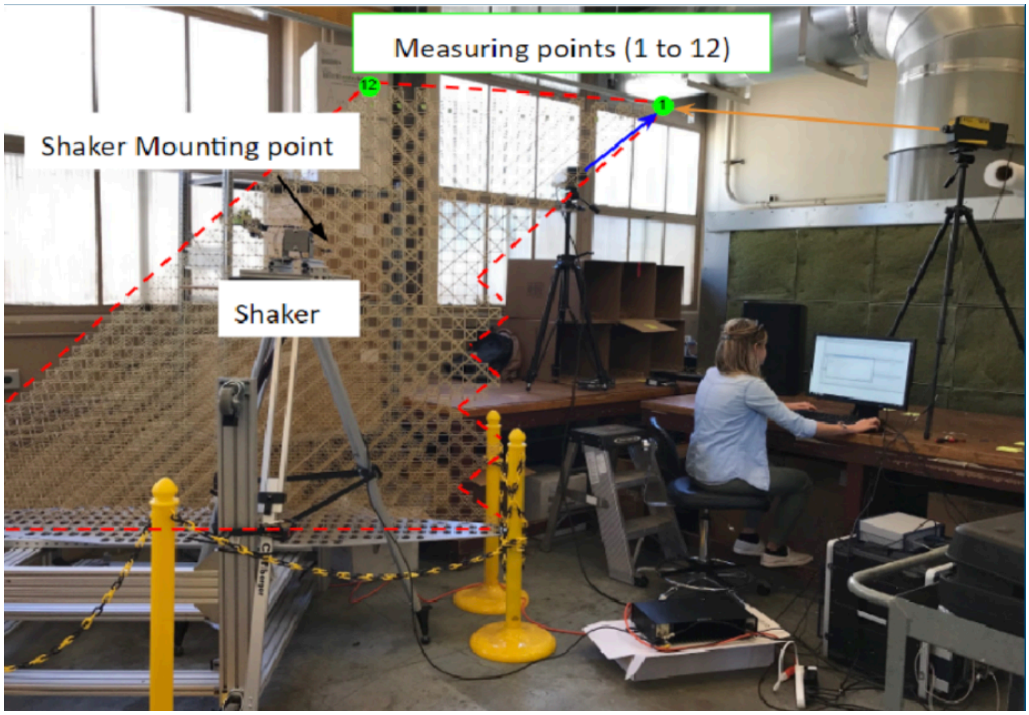

Figure 14: Experimental Setup

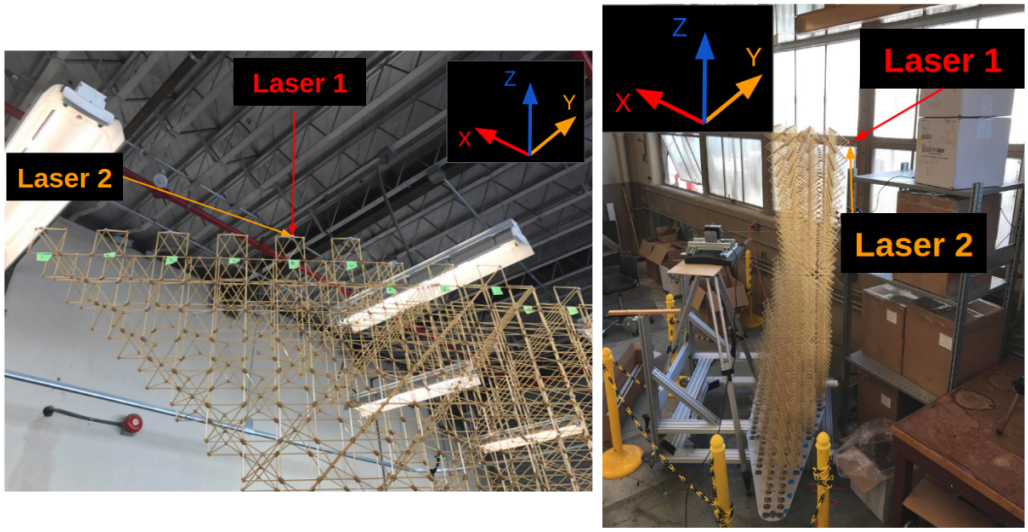

Figure 15: Lasers Setup on Wing Structure

From the experiments, the first mode of vibration has the natural frequency at 10.31 Hz, detected on the measuring points 1 and 12 on the Y axis (figure 16).

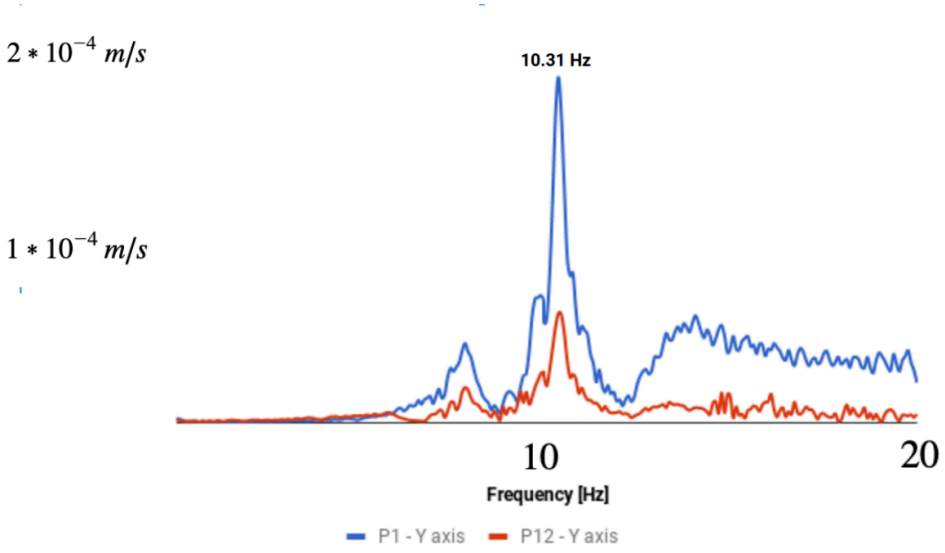

Figure 16: First mode of vibration

The second mode of vibration is caught at 27 Hz on both Y and Z axis from the measuring points 1, 5, 9 and 12 (figure 17).

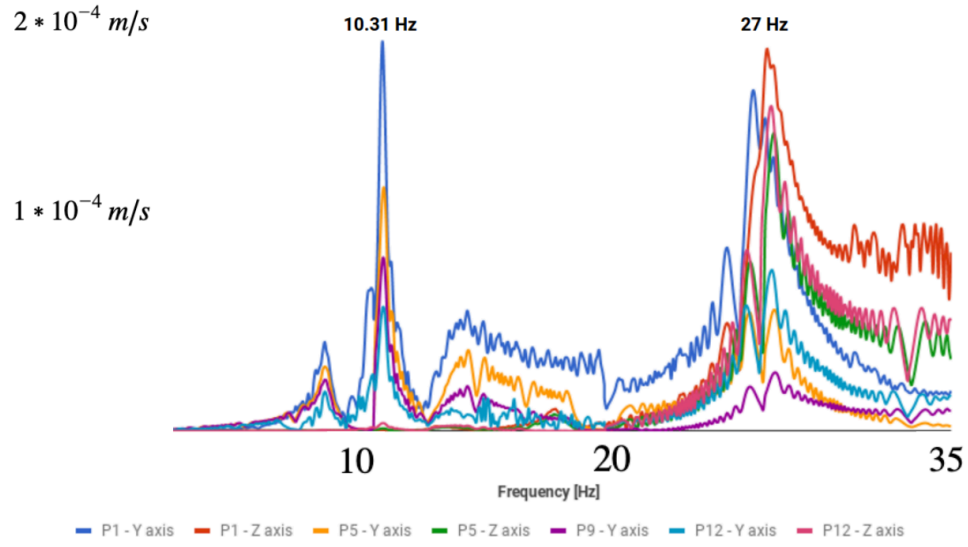

Figure 17: Second mode of vibration

Third mode of vibration is detected at 30.31 Hz on the Z axis from the measuring points 9 and 12 (figure 18).

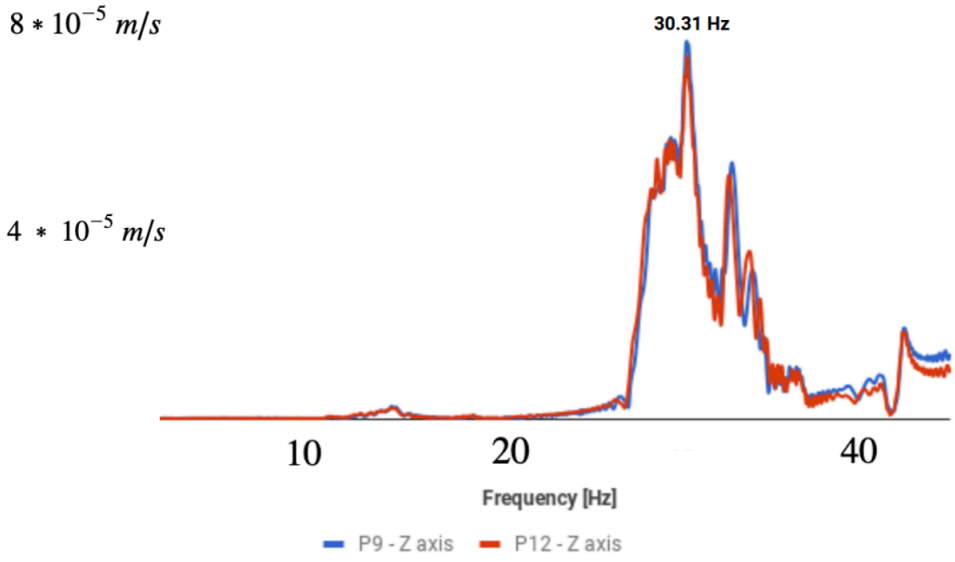

Figure 18: Third mode of vibration

The fourth mode of vibration is caught at 49.5 Hz on measuring point 5 from the Z direction and at 41 Hz on point 9 and point 12 (figure 19).

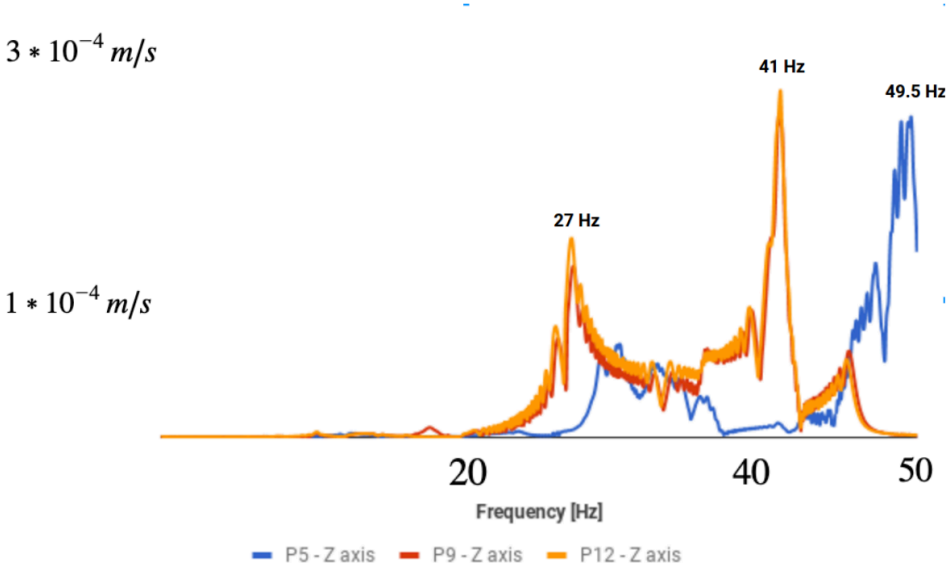

Figure 19: Fourth mode of vibration

The fifth mode of vibration is caught at 58 Hz on the measuring point 12 from

the Z direction (fig. 20).

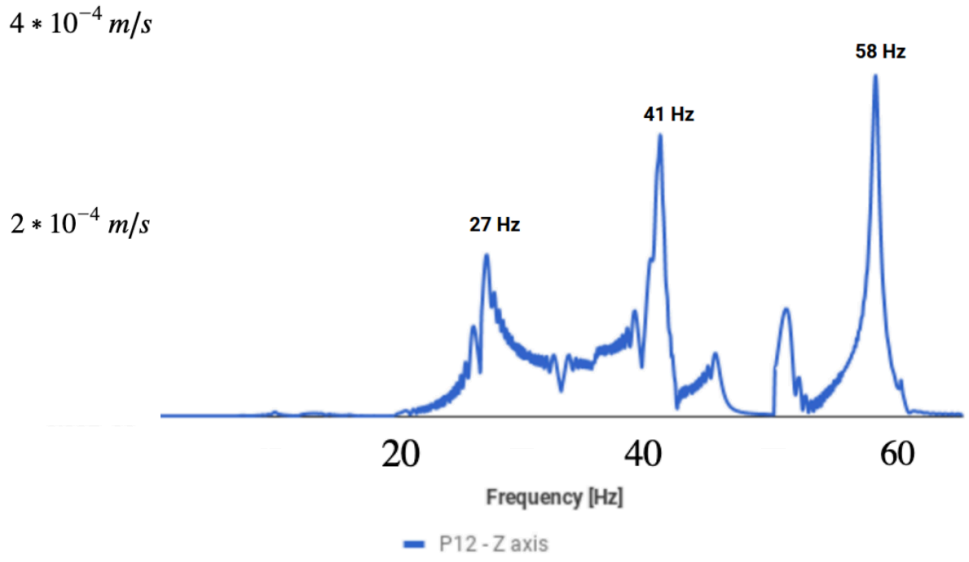

Figure 20: Fifth mode of vibration

The seventh mode of vibration is caught at 84 Hz on the Z axes on the measuring point 9 (figure 21).

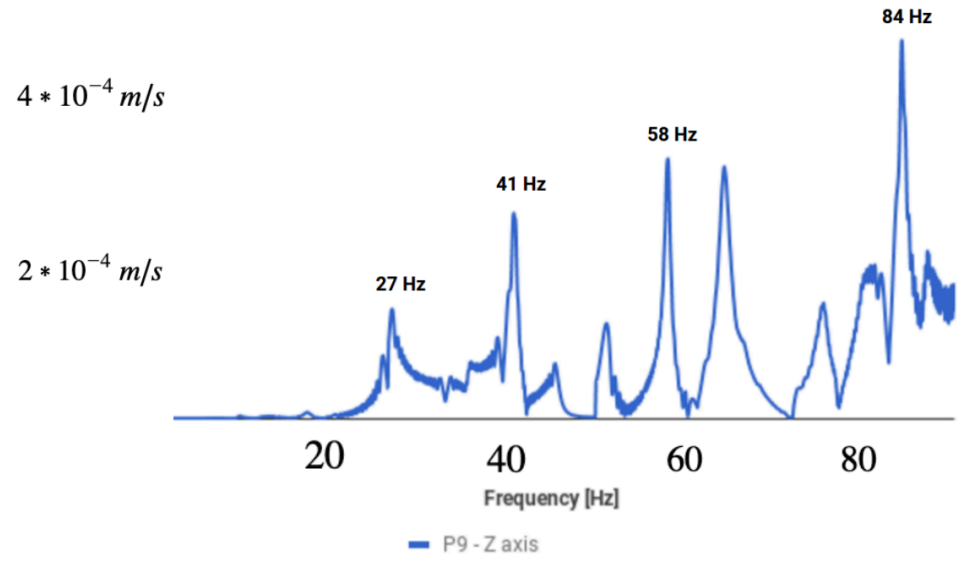

Figure 21: Seventh mode of vibration

To summarize the laser vibrometer technique, the results of the vibrometer laser measurements are shown in table 1:

	Experiment
	Frequency[Hz]
1st mode	10.31
2nd mode	27
3rd mode	30.31
4th mode	49.5
5th mode	58
6th mode	-
7th mode	84

Table 1: Experimental Analysis

4.2 Analytical Model of Morphing Wing

4.2.1 Dynamic Stiffness Method

Working with an aircraft wing, we tried to represent the wing as a bending-torsion coupled beam. The coupling between the bending and torsional motions is developed from the non-coincident elastic and mass axes of the wing. The model of partial differential equations of motion of bending-torsion wing is the following:

$$EIh''' + m\ddot{h} - mx_\alpha\ddot{\psi} = 0$$

$$GJ\ddot{\psi} + mx_\alpha\ddot{h} - I_\alpha\ddot{\psi} = 0$$

where EI and GJ are the bending and torsional rigidities of the wing, m is the mass per unit length, I the polar mass moment of inertia per length about the Y-axis and the partial differentiation with respect to position y and time t.

After processing the equations, the frequency dependent dynamic stiffness matrix K is given by:

$$K = DB^{-1}$$

We could model the wing with the dynamic stiffness matrix equation, representing the bending-torsion coupled beam. Since the wing is not uniform, it can be modelled as an assembly of many uniform dynamic stiffness elements. The wing was split in 5 elements with same material properties, but different geometry dimensions. The overall dynamic stiffness matrix of the complete wing is assembled from each of the 5 dynamic stiffness elements.

In order to extract the natural frequencies and mode shapes from the overall dynamic stiffness matrix of the wing, the Wittrick-Williams algorithm [8] is applied, which has featured in hundreds of papers. The algorithm is particularly suitable in solving free vibration problem using the dynamic stiffness method.

The algorithm monitors the Sturm sequence condition of the overal stiffness matrix K, in such a way that there is no possibility of missing any natural frequency of the wing. We summarise the procedure of the algorithm next.

Suppose that ω denotes the circular (or angular) frequency of the vibrating wing. According to the Wittrick-Williams algorithm, j, the number of natural frequencies passed, as ω is increased from zero to ω^*, is given by:

$$j = j_0 + sK$$

sK is the number of negative elements on the leading diagonal of $K^{\triangle}$, $K^{\triangle}$ is the upper triangular matrix obtained by applying the usual form of Gauss elimination to K, and j0 is the number of natural frequencies of the wing still lying between ω =0 and $\omega = \omega^*$, when the displacement components to which K corresponds are all zeros.

Therefore, it can be determined how many natural frequencies of the wing lie below an arbitrarily chosen trial frequency:

$$j_0 = \sum j_m$$

The algorithm was implemented in a FORTRAN executable program, called CALFUN, which calculates the flutter speed of an unswept cantilever aicraft wing using finite element method and two dimensional unsteady aerodinamics. The normal approach through the use of generalised coordinates is implemented for the wing to be idealised both aerodinamically and structurally. The beam element representation of the wing stands for the structural idealisation, while the strip theory based on the Theodorsen expression for lift and moment stands for the aerodinamic idealisation. The flutter matrix is formed by algebraically summing the mass, stiffness and aerodinamic matrices.

The data necessary for the vibration analysis is the bending rigidity, the torsional rigidity, the mass per unit length, polar mass moment of inertia per unit length, the distance between elastic axis and mass axis and the length of the wing or elements. The elastic axis was considered to coincide with the Y-axis. The FORTRAN program provided the natural frequencies of the first 4 modes of vibration only, provided in the following table (table 2):

	Experiment	DSM	
	Frequency[Hz]	Frequency[Hz]	Error
1st mode	10.31	100.49	874.68%
2nd mode	27	150.56	457.66%
3rd mode	30.31	276.82	813.3%
4th mode	49.5	450.7	810.51%

Table 2: DSM & Experimental Analysis

After analysing the results and comparing them with the laser vibrometer measurements, it was proven that the dynamic stiffness method does not represent a suitable approach for the aircraft wing in our case, since the wing is not a high aspect ratio wing and idealising it as a beam of 5 or more elements does not validate this method.

4.2.2 Rectangular Plate Model

There is a large literature for free vibration of rectangular plates. The basic theory of rectangular plates is defined by the following differential equation:

$$D\nabla^4 w + \rho\frac{\partial^2 w}{\partial t^2} = 0$$

, where w is transverse deflection; ∇^4 is the biharmonic differential operator, and D represents the flexural rigidity:

$$D = \frac{Eh^3}{12(1-\nu^2)}$$

E is Young's modulus; h is plate thickness; ν is Poisson's ratio; ρ is mass density per unit area of plate surface; and t is time [24].

In our case, the wing is considered to be a rectangular plate clamped at the base edge, while all the other 3 edges are considered to be free.

Let consider the wing as a rectangular thin plate with dimension of a (m) by b(m) and h(m) thick [3]. Based on the principle of virtual work, the steady state transverse displacement, $\xi_0(x,y)$ of a clamped rectangular plate at the point excitation $(x^{'}, y^{(\prime)})$

$$\xi_0(x,y) = F_0\sum_{m=1}^{\infty}\sum_{n=1}^{\infty}\frac{\Psi_{mn}(x,y)\Psi_{mn}\left(x',y'\right)}{B\left(I_1I_2+2I_3I_4+I_5I_6\right)-\rho_s\omega^2I_2I_6}$$

The shape function is given as:

$$\Psi_{mn}(x,y) = \vartheta_m(x)\zeta_n(y)$$

, where:

$$\vartheta_m(x) = \mathcal{J}\left(\beta_m x/a\right) - \frac{\mathcal{J}\left(\beta_m\right)}{\mathcal{H}\left(\beta_m\right)}\mathcal{H}\left(\frac{\beta_m x}{a}\right)$$

$$\mathcal{J}(s) = \cosh(s) - \cos(s)$$

$$\mathcal{H}(s) = \sinh(s) - \sin(s)$$

$$\zeta_n(y) = \mathcal{J}\left(\beta_n y/b\right) - \frac{\mathcal{J}\left(\beta_n\right)}{\mathcal{H}\left(\beta_n\right)}\mathcal{H}\left(\beta_n y/b\right)$$

Numerical results for the dimensionless frequency parameter:

$$\lambda = \omega a^2 \sqrt{\frac{\rho}{B}}$$

were computed using the following equation:

$$\omega_{mn} = \sqrt{\frac{B}{\rho_s}} \sqrt{\left(\frac{\beta_m}{a}\right)^4 + \left(\frac{\beta_n}{b}\right)^4 + 2\left(\frac{\beta_m \beta_n}{ab}\right)^2 \frac{R_m R_n}{2_m 2_n}}$$

, for rectangular plates of arbitrary a/b ratio.

The model implementation was created in Matlab and all the numerical results were computed, from the a/b ratio to the natural frequencies of the rectangular idealised wing plate. The results are presented in table 3.

	Experiment	Rectangular plate	
	Frequency[Hz]	Frequency[Hz]	Error
1st mode	10.31	29.67	187.78%
2nd mode	27	51.61	91.148%
3rd mode	30.31	87.31	188.06%
4th mode	49.5	36.857	25.541%
5th mode	58	196.88	239.45%
6th mode	-	273.50	-
7th mode	84	350	316.67%

Table 3: Rectangular Plate Model & Experimental Analysis

4.2.3 Trapezoidal Plate Model

In the present study, the wing is idealised as a trapezoidal plate made of ULTEM 2200 plate having a base width a = 3.619 m, top width b = 1.848 m, height d = 2.849 m and thickness h = 0.539 m to h = 0.308 m, and having the following material properties: the modulus of elasticity E = 2.57 MPa, Poisson's ratio $\nu = 0.35$ and density $\rho = 259.74kg/m^3$.

The results are influenced by the free-width ratio, the clamped position, and the swept-back angle on the vibrations of the trapezoidal plate [8]. The natural frequency (circular frequency) ω is expressed in terms of a dimensionless frequency parameter λ:

$$\lambda = \omega a^2 \left(\frac{\rho h}{D}\right)^{1/2}$$

D is the flexural rigidity of the trapezoidal plate, defined as:

$$D = \frac{Eh^3}{12\left(1 - v^2\right)}$$

The dimensionless frequency parameter was determined in previous studies and experiments, based on the plate geometrical form, free-width ratio, summarized in tables based on boundary conditions [38].

The natural frequencies of plates increase linearly with thickness and decrease inversely with a^2 length [5].

The dimensionless frequency parameter λ is a function of the boundary conditions, plate geometry and Poisson's ratio for free boundary conditions:

$$\lambda = \lambda(\textit{boundary conditions, geometry, Poisson's ratio})$$

So, the natural frequency can be expressed as:

$$\omega_{ij} = \frac{\lambda_{ij}^2}{2\pi a^2}\sqrt{\frac{Eh^3}{12\gamma\left(1-v^2\right)}}$$

The aircraft wing is idealised here as an asymmetric simply supported trapezoidal plate:

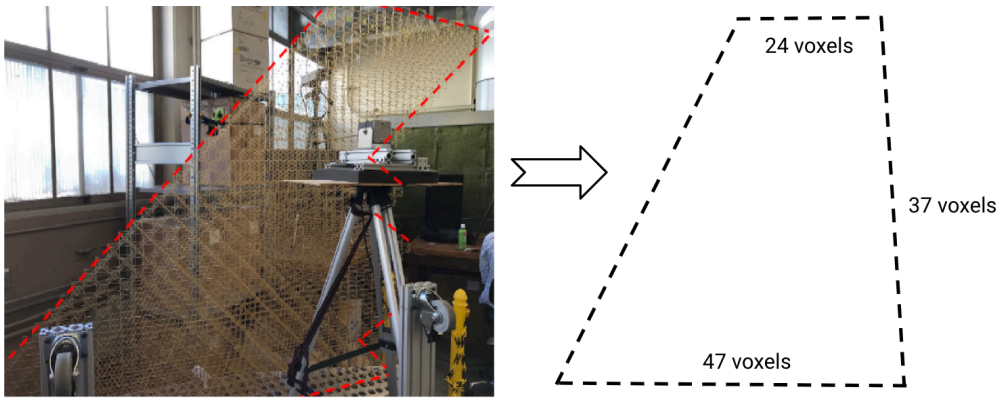

Figure 22: Trapezoidal plate - Wing sketch

We can determine from the wing dimensions the following: $b/a = 0.51$ and $d/a = 0.787$.

Regarding the results obtained in earlier studies [5], the dimensionless frequency parameter was obtained through the method of linear interpolation of the dimensionless parameter λ, from the determined values for general cases:

Wing lengths ratio			
b/a	d/a=0.5	d/a=1.0	d/a=1.5
0.4	64.26	32.50	25.39
0.8	52.47	23.18	17.86

Table 4: Dimensionless frequency parameter - Wing ratios

Obtaining the fundamental parameter $\lambda = 6.5710$ through interpolation and based on plate analysis of eigenvalues of vibration of several methods [19], [13], [31], we could determine the dimensionless frequency parameters of each vibra-

tion mode in our case.

Therefore, natural frequencies of each mode of vibration were determined based on this method and the results are shown in the following table (table 5):

	Experiment	Trapezoidal plate	
	Frequency[Hz]	Frequency[Hz]	Error
1st mode	10.31	9.35	9.29%
2nd mode	27	12.882	52.28%
3rd mode	30.31	30.536	0.74%
4th mode	49.5	36.857	25.541%
5th mode	58	47.95	17.327%
6th mode	-	73.118	-
7th mode	84	78.605	6.4233%

Table 5: Trapezoidal Plate Model & Experimental Analysis

An important discussion for the current method is represented by the parameters variations, for example: the modulus of elasticity, wing thickness or density.

The wing thickness goes from 0.539 m on the base of the wing to 0.308 m on the highest level of the wing. The difference in the natural frequencies is shown in figure 23.

The material ULTEM 2200 has modulus of elasticity and density that influences the behavior as well. The error bar are shown in the plots in figures 24 and 25.

It can be easily perceived from the plot in figure 26 that the trapezoidal plate method is the one that is validating the experimental results.

The conclusion of the most accurate analytical method implemented can be drawn from table 6:

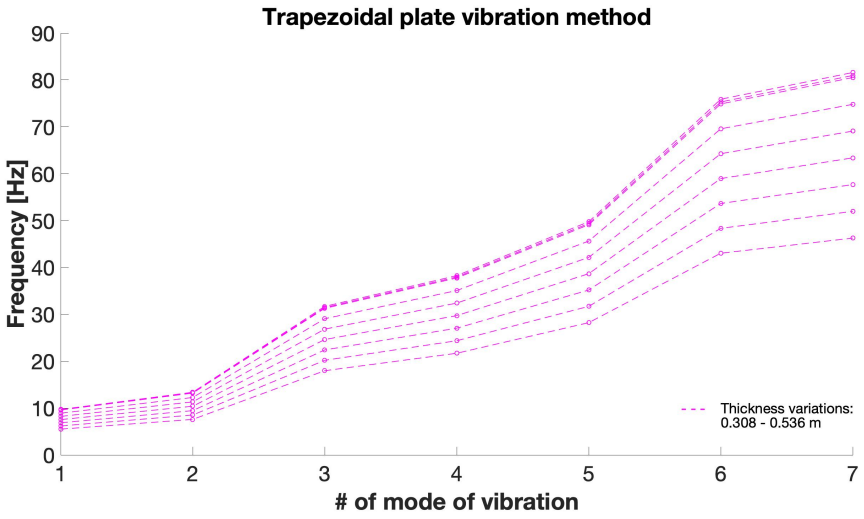

Figure 23: Trapezoidal plate vibration method - Thickness variations

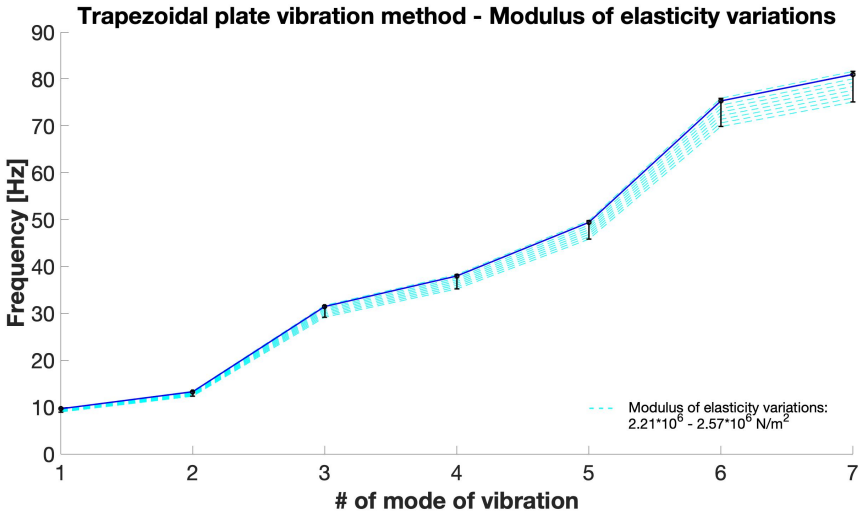

Figure 24: Trapezoidal plate vibration method - Modulus of elasticity variations

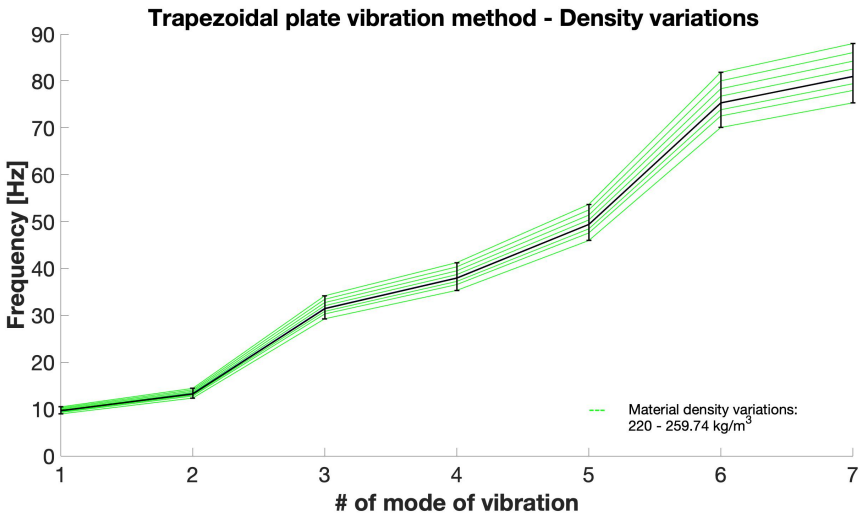

Figure 25: Trapezoidal plate vibration method - Density variations

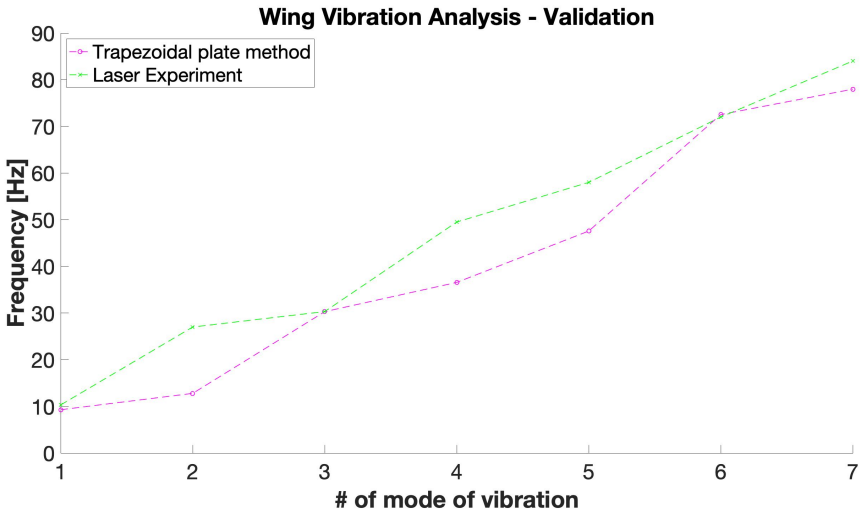

Figure 26: Trapezoidal plate vibration method - Validation with experiment

	Experiment	Trapezoidal plate		Rectangular plate		DSM	
	Frequency[Hz]	Frequency[Hz]	Error	Frequency[Hz]	Error	Frequency[Hz]	Error
1st mode	10.31	9.35	9.29%	29.67	187.78%	100.49	874.48%
2nd mode	27	12.882	52.28%	51.61	91.148%	150.568	457.66%
3rd mode	30.31	30.536	0.7442%	87.31	188.06%	276.82	813.33%
4th mode	49.5	36.857	25.541%	135.86	174.46%	450.7	810.51%
5th mode	58	47.95	17.327%	196.88	239.45%	-	-
6th mode	-	73.118	-	273.50	-	-	-
7th mode	84	78.605	6.4233%	350	316.67%	-	-

Table 6: Aircraft lattice wing - Analytical methods

4.3 FEA Simulation

In order to validate the use of the beam modeling approach for digital material substructures as a means of reduced order simulation a fully meshed Abaqus finite element model was run for a single voxel. Figure 27 shows the Abaqus tetrahedron mesh which contains 12 217 nodes and 6 019 elements. The bottom most node was constrained to only axial movement in the vertical direction to replicate the experimental set-up which will be presented later. Using the single

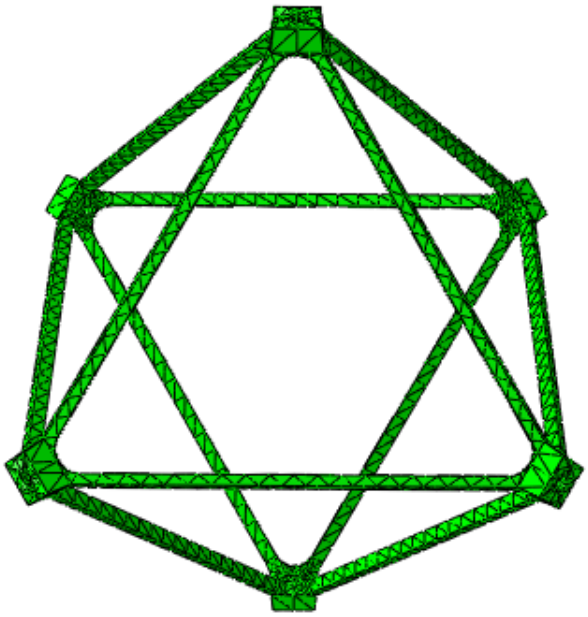

Figure 27: Abaqus cubic octrohedron volumetric pixel tetrahedron mesh

beam voxel presented earlier, the wing substructure in figure 28 can be simulated with, 13 0752 nodes and 148 425 elements.

With the same tetrahedral mesh that was used before, that would result in a total of 2.5509096e7 and 1.2567672e7 elements, which is too large of a simulation to solve in a reasonable amount of time and would preclude eventual optimization or aeroelastic analysis (figure 29). The furthest inboard nodes had the fully fixed encaster boundary condition applied to them and the Eigen Solver Lanczos method was used.

Figure 28: Wing voxel substructure

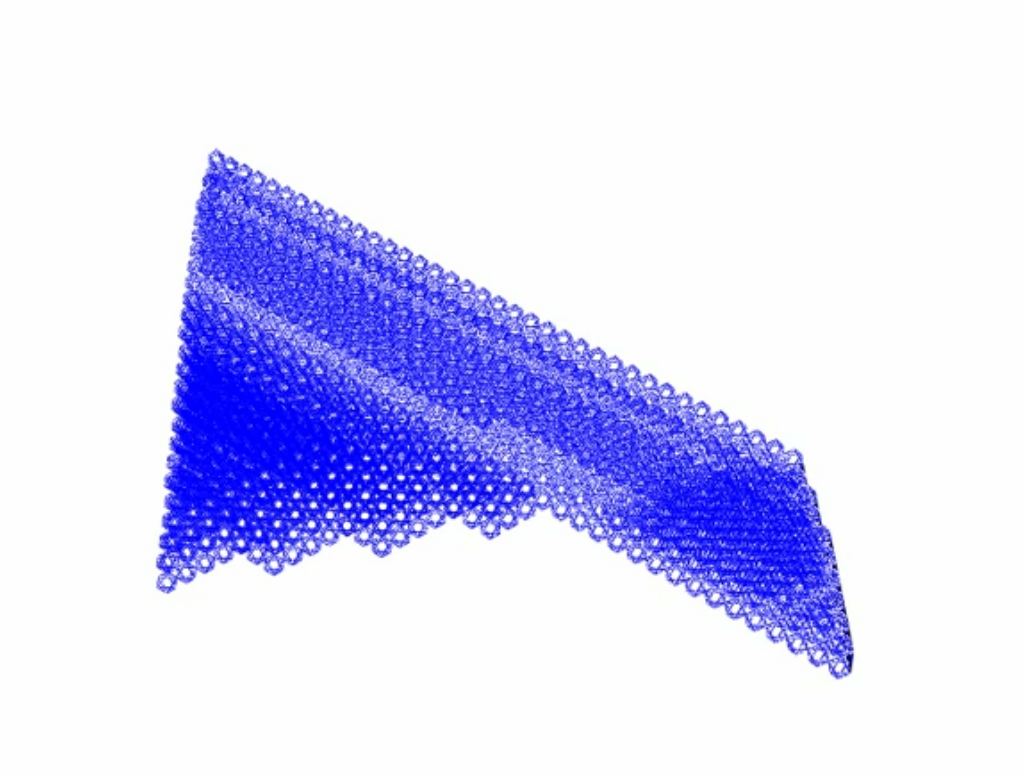

Figure 29: Abaqus wing mesh

Abaqus shows that the first mode of vibration has a frequency of 9.0788 Hz (figure 30). The second mode of vibration in Abaqus shows a frequency of 26.166 Hz (figure 31). The third mode of vibration shows a frequency of 31.160 Hz

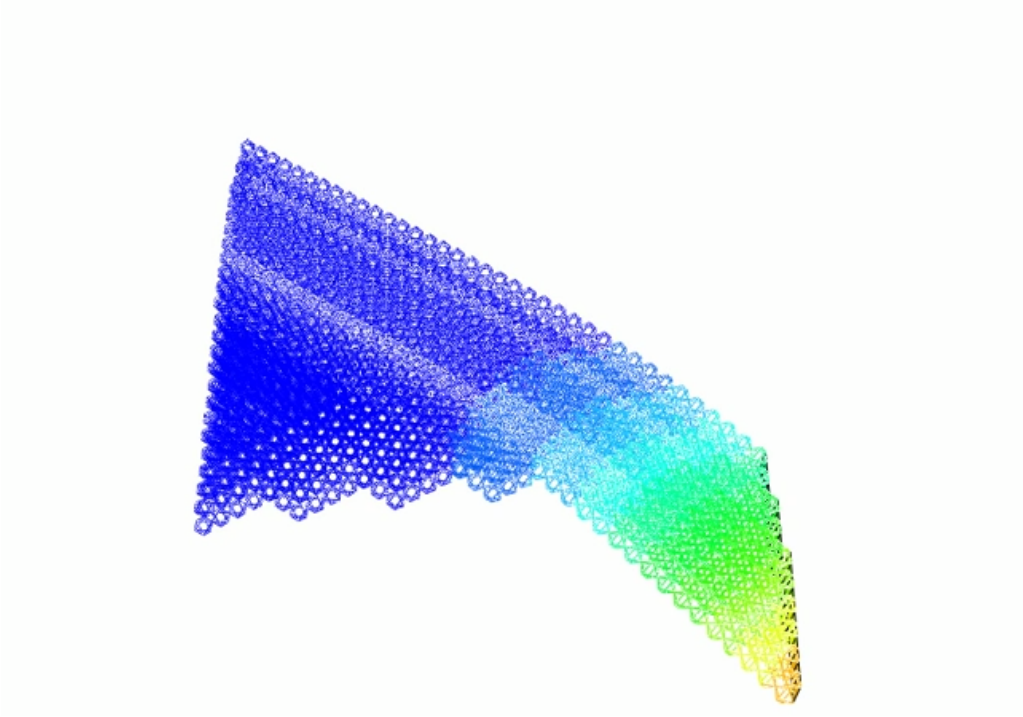

Figure 30: Abaqus Wing Simulation - first mode of vibration

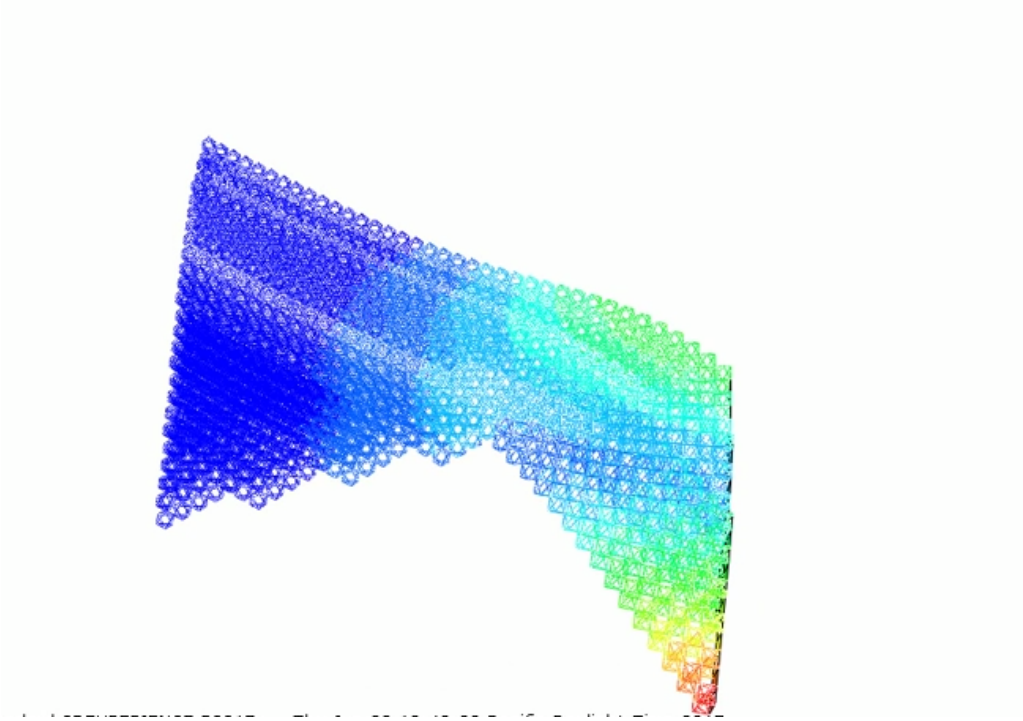

Figure 31: Abaqus Wing Simulation - second mode of vibration

(figure 32). The fourth mode of vibration shows a frequency of 47.177 Hz (figure 33). The fifth mode of vibration shows a frequency of 57.259 Hz (figure 34). The

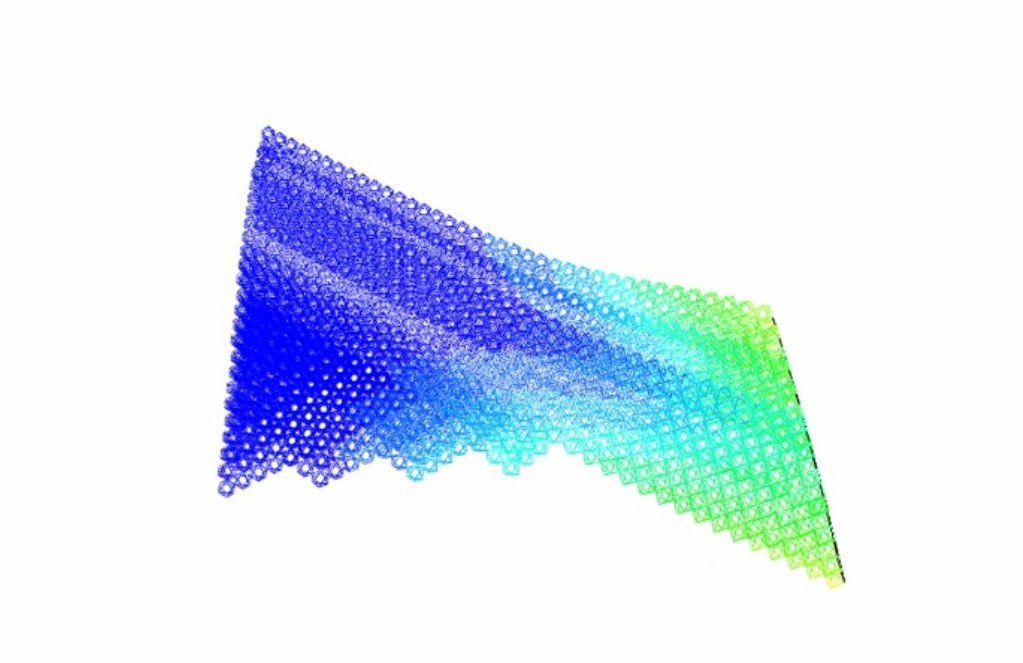

Figure 32: Abaqus Wing Simulation - third mode of vibration

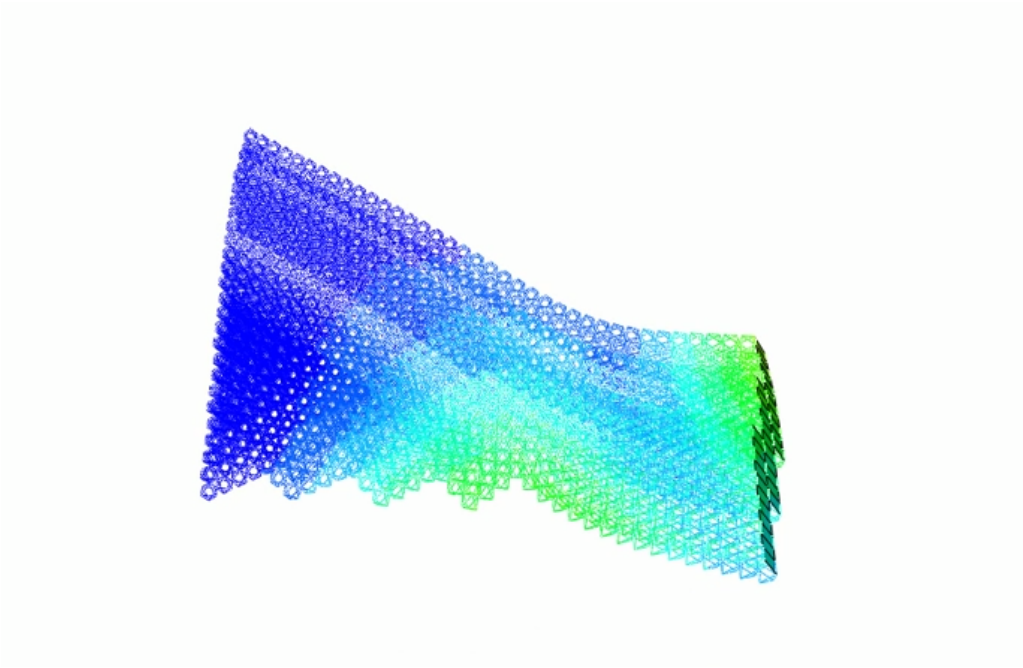

Figure 33: Abaqus Wing Simulation - fourth mode of vibration

sixth mode of vibration shows a frequency of 73.647 Hz (figure 35). The seventh mode of vibration shows a frequency of 81.073 Hz (figure 36).

The simulation results are presented in table 7.

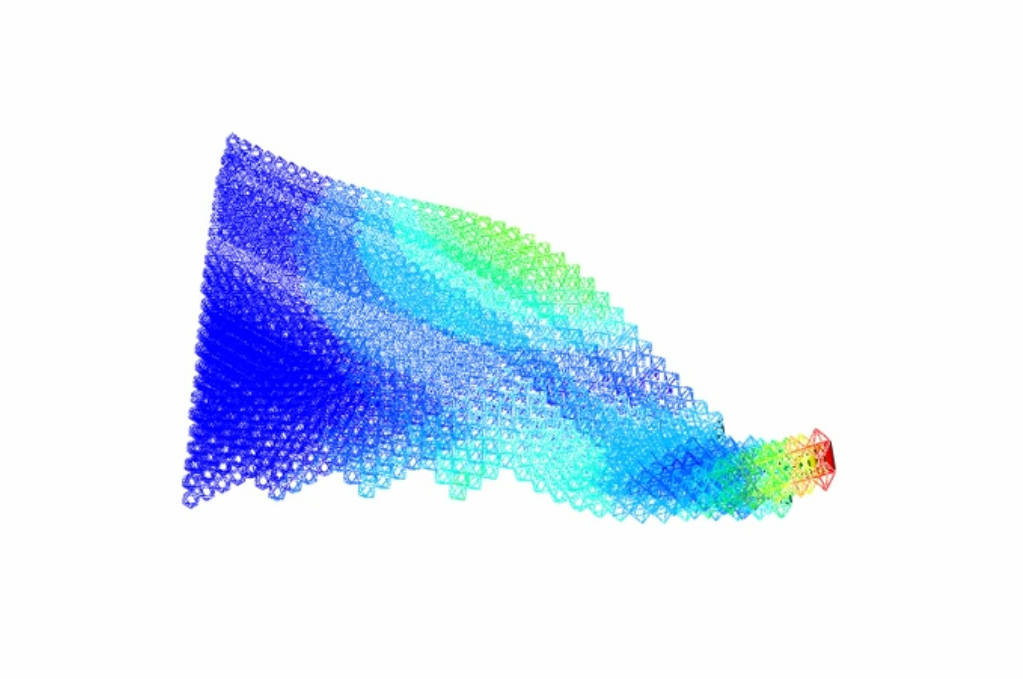

Figure 34: Abaqus Wing Simulation - fifth mode of vibration

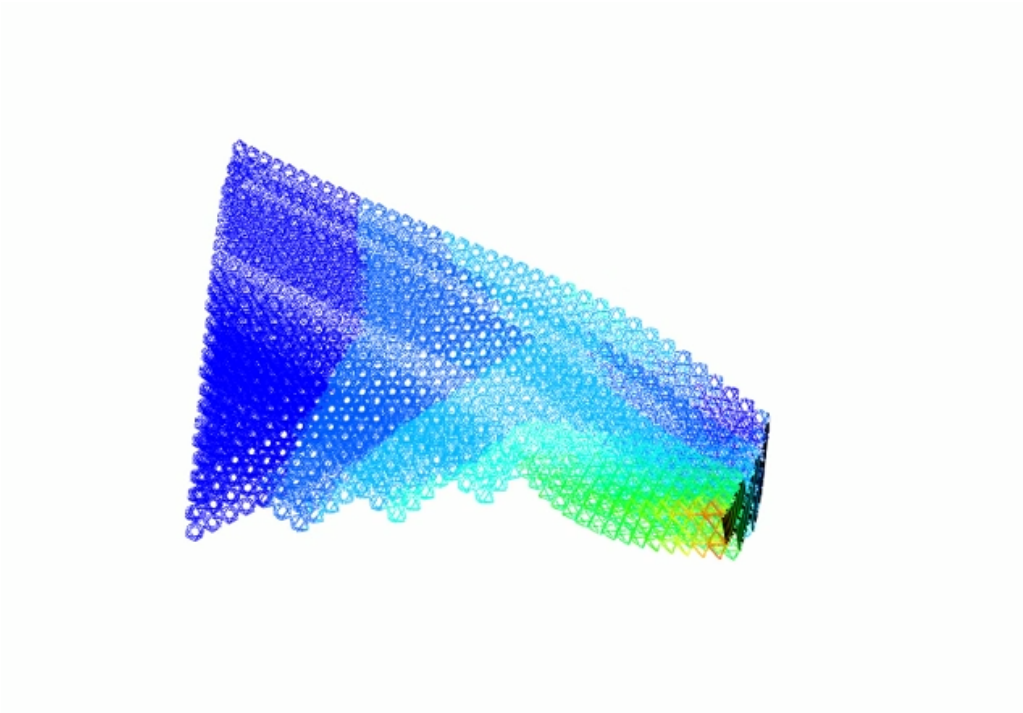

Figure 35: Abaqus Wing Simulation - sixth mode of vibration

The study proves the methods implemented for ultra-light lattice structures are valid and their accuracy cannot be denied. The entire set of results is presented

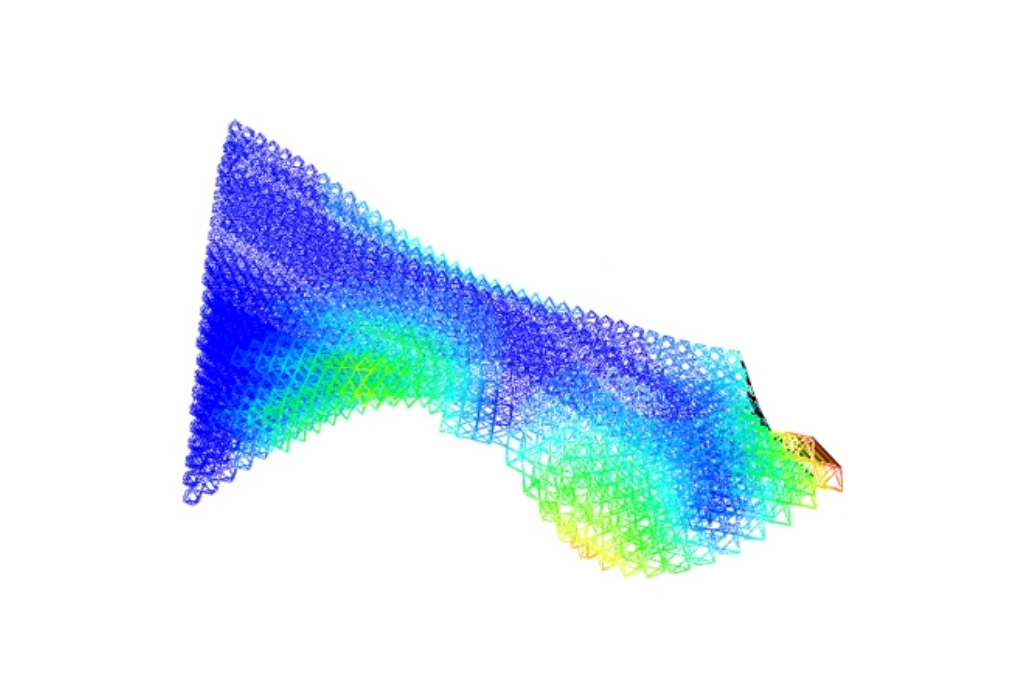

Figure 36: Abaqus Wing Simulation - seventh mode of vibration

	Simulation
	Frequency[Hz]
1st mode	9.0788
2nd mode	26.166
3rd mode	31.160
4th mode	47.177
5th mode	57.259
6th mode	73.647
7th mode	81.073

Table 7: Morphing Wing - ABAQUS Simulation

in table 8:

	Experiments	Simulation	Trapezoidal plate		Rectangular plate		DSM	
	Frequency[Hz]	Frequency[Hz]	Frequency[Hz]	Error	Frequency[Hz]	Error	Frequency[Hz]	Error
1st mode	10.31	9.0788	9.35	9.29%	29.67	187.78%	100.49	874.48%
2nd mode	27	26.166	12.882	52.28%	51.61	91.148%	150.568	457.66%
3rd mode	30.31	31.16	30.536	0.7442%	87.31	188.06%	276.82	813.33%
4th mode	49.5	47.177	36.857	25.541%	135.86	174.46%	450.7	810.51%
5th mode	58	57.259	47.95	17.327%	196.88	239.45%	-	-
6th mode	-	73.647	73.118	-	273.50	-	-	-
7th mode	84	81.073	78.605	6.4233%	350	316.67%	-	-

Table 8: Aircraft lattice wing - Final results

Furthermore, for the readers understanding, the results are represented in the following plots as well (figure 37 and figure 38). In figure 37 it is shown that the trapezoidal method validates the approach, while figure 38 shows the overall analysis of this study.

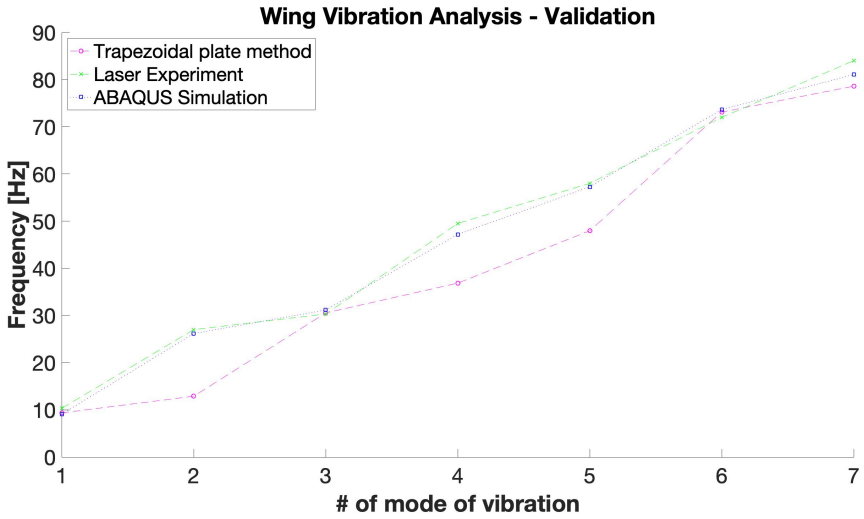

Figure 37: Model - Experiment - Simulation Validation

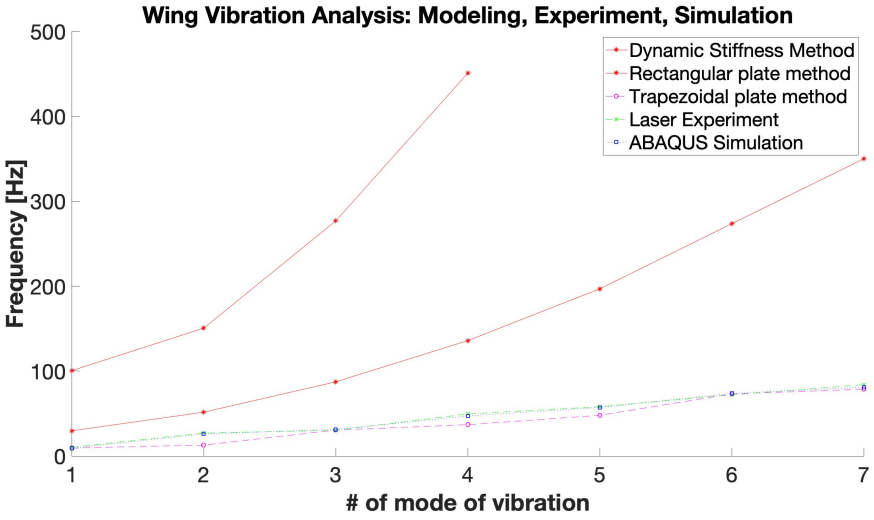

Figure 38: Model - Experiment - Simulation Analysis

5 Conclusions

The purpose of this study was to investigate the vibrations and the natural frequencies of a base-excitation modal testing technique for a lattice based aeroelastic wing.

Vibration analysis of an aircraft wing created from lattice structures is essential and the work in this thesis provided that vibration analysis experimentally and then verified analytically. The components of this investigation were:

1. Introduction of the concept of a volumetric pixel and then the modular lattice structure used to build the aircraft wing

2. Creation of the experimental setup required to employ the laser vibrometer testing technique. The experimental vibration analysis was carried out by design and implementation of a laser vibrometer setup for this testing. The ultra-light structures in this experimental setup are vibrated by a shaker, which induces translational motion in the lateral direction of the wing. One or two vibrometer lasers detect the natural frequencies of the vibrations created by the shaker.

3. Determination of the natural frequencies of each lattice block, starting with analysis of one single volumetric pixel and then the aircraft wing composed of these pixels, via measurements made using the experimental setup.

4. Development of an analytical model of the experimental setup used for measurement of the wing, and also via finite element frequency analysis using a computer-aided design tool. These followed from the introduction of digital meta materials in order to understand volumetric pixels and then used to understand various lattice structures derived from them.

5. Validation of the experimental measurements through analytical modeling, focused on the natural frequencies of the system of equations developed,

which were based on geometry, boundary conditions and material properties.

6. Validation of the experimental and analytical results via a finite element analysis made using the computer-aided design tool ABAQUS.

The detected natural frequencies and mode shapes are in good agreement across the experiments, the analytical findings and simulation procedure.

As final approach to the current problem, the experimental results and analytical results were validated as well through a finite element analysis in the computer aided design tool Abaqus. The detected natural frequencies and mode shapes are in good agreement from the experiments, numerical findings and simulation procedure.

The main finding of the study can be summarized as follows: experimental and analytical methods for vibration analysis of discretely assembled ultra-light structures, which are common in various aircraft applications (and in other craft), provide useful results. Specifically, the validity and accuracy of the general laser experimental method developed and used in this work was demonstrated via analytical modeling and by application of finite element analysis to detect natural frequencies and mode shapes.

6 Future Work

Future research suggested by this study include:

1. Modeling of the morphing wing as a combination of plate and beam, after analyzing the modes from the simulations that show the wing behaves similar to a plate with a beam attached

2. Further investigation and analysis of the implications of boundary conditions

3. Further investigation of the geometry and forces and how they affects the aircraft wing performance

4. Study of new implementations of different types of digital meta materials for the same aircraft application

5. Investigation of different materials and comparison of the results with those of this study

6. Design and implementation of a control system appropriate for an aircraft with a lattice based aeroelastic wing that would enable autonomous flying

References

[1] Mark Adel, Khalil Ibrahim, Abdel-Rassoul Gad, and Abo El-Makarem Khalil. Development of dynamic model for vibration control of flexible beam. 2016.

[2] Bilel Aidi, Mohamed Shaat, Abdessattar Abdelkefi, and Scott W Case. Free vibration analysis of cantilever open-hole composite plates. *Meccanica*, pages 1–18.

[3] Jorge P Arenas. On the vibration analysis of rectangular clamped plates using the virtual work principle. *Journal of Sound and Vibration*, 266(4):912–918, 2003.

[4] Steven M Arnold, David Cebon, and Mike Ashby. Materials selection for aerospace systems. 2012.

[5] Robert D Blevins. *Formulas for dynamics, acoustics and vibration*. John Wiley & Sons, 2015.

[6] Daniel Cellucci, Benjamin Jenett, and Kenneth C Cheung. Digital cellular solid pressure vessels: A novel approach for human habitation in space. In *Aerospace Conference, 2017 IEEE*, pages 1–7. IEEE, 2017.

[7] TERRY CHEN. Experimental and numerical studies of the transverse vibration of partially clamped trapezoidal plates. *Chinese Society of Mechanical Engineers, Journal*, 11:301–307, 1990.

[8] TY Chen, WR Wang, JJ Ju, and SY Lee. Free vibrations of a partially clamped trapezoidal plate. *Experimental mechanics*, 35(1):49–54, 1995.

[9] Kenneth C Cheung and Neil Gershenfeld. Reversibly assembled cellular composite materials. *science*, 341(6151):1219–1221, 2013.

[10] Kenneth Chun-Wai Cheung. *Digital cellular solids: Reconfigurable composite materials*. PhD thesis, Massachusetts Institute of Technology, 2012.

[11] I Chopra and S Durvasula. Vibration of simply-supported trapezoidal plates i. symmetric trapezoids. *Journal of Sound and Vibration*, 19(4):379–392, 1971.

[12] I Chopra and S Durvasula. Vibration of simply-supported trapezoidal plates ii. unsymmetric trapezoids. *Journal of Sound and Vibration*, 20(2):125–134, 1972.

[13] RW Claassen. Vibrations of skew cantilever plates. *AIAA Journal*, 1(5):1222–1222, 1963.

[14] Nick Cramer, Sean Shan-Min Swei, Kenneth C Cheung, and Mircea Teodorescu. Extended discrete-time transfer matrix approach to modeling and decentralized control of lattice-based structures. *Structural Control and Health Monitoring*, 23(10):1256–1272, 2016.

[15] Andrea Cusano, Patrizio Capoluongo, S Campopiano, Antonello Cutolo, Michele Giordano, Ferdinando Felli, Antonio Paolozzi, and Michele Caponero. Experimental modal analysis of an aircraft model wing by embedded fiber bragg grating sensors. *IEEE Sensors Journal*, 6(1):67–77, 2006.

[16] R Ganesh and Stefano Gonella. Experimental evidence of directivity-enhancing mechanisms in nonlinear lattices. *Applied Physics Letters*, 110(8):084101, 2017.

[17] Christine E Gregg, Joseph H Kim, and Kenneth C Cheung. Ultra-light and scalable composite lattice materials. *Advanced Engineering Materials*, 20(9):1800213, 2018.

[18] Myungwon Hwang and Andres F Arrieta. Nonlinear dynamics of bi-stable lattices with defects. In *SPIE Smart Structures and Materials+ Nondestructive Evaluation and Health Monitoring*, pages 101701A–101701A. International Society for Optics and Photonics, 2017.

[19] Toshihiro Irie, Gen Yamada, and Hajime Ida. Free vibration of a stiffened trapezoidal cantilever plate. *The Journal of the Acoustical Society of America*, 72(5):1508–1513, 1982.

[20] Benjamin Jenett, Sam Calisch, Daniel Cellucci, Nick Cramer, Neil Gershenfeld, Sean Swei, and Kenneth C Cheung. Digital morphing wing: active wing shaping concept using composite lattice-based cellular structures. *Soft Robotics*, 4(1):33–48, 2017.

[21] Benjamin Jenett, Daniel Cellucci, Christine Gregg, and KC Cheung. Meso-scale digital materials: modular, reconfigurable, lattice-based structures. In *Proceedings of the 2016 Manufacturing Science and Engineering Conference*, 2016.

[22] H Kato. On the bending and vibration of rectangular plates. *Journal of Zosen Kiokai*, 1932(50):209–230, 1932.

[23] PAA Laura, RH Gutierrez, and RB Bhat. Transverse vibrations of a trapezoidal cantilever plate of variable thickness. *AIAA journal*, 27(7):921–922, 1989.

[24] Arthur W Leissa. The free vibration of rectangular plates. *Journal of sound and vibration*, 31(3):257–293, 1973.

[25] AW Leissa. Recent studies in plate vibrations: 1981-1985. part 2: Complicating effects. *Vibration Inst., The Shock and Vibration Digest*, 19(3):10–24, 1987.

[26] Ata Mahjoubfar, Claire Lifan Chen, and Bahram Jalali. Nanometer-resolved imaging vibrometer. In *Artificial Intelligence in Label-free Microscopy*, pages 15–20. Springer, 2017.

[27] K Maruyama, O Ichinomiya, and Y Narita. Experimental study of the free vibration of clamped trapezoidal plates. *Journal of Sound and Vibration*, 88(4):523–534, 1983.

[28] MI McEwan, Jan R Wright, Jonathan E Cooper, and Andrew Yee Tak Leung. A combined modal/finite element analysis technique for the dynamic response of a non-linear beam to harmonic excitation. *Journal of Sound and Vibration*, 243(4):601–624, 2001.

[29] Kevin Napolitano and Daniel Linehan. Multiple sine sweep excitation for ground vibration tests. *IMAC XXVII, Orlando, Florida*, 2009.

[30] Ruth M Orris and M Petyt. A finite element study of the vibration of trapezoidal plates. *Journal of Sound and Vibration*, 27(3):325–344, 1973.

[31] MN Bapu Rao, P Guruswamy, M Venkateshwara Rao, and S Pavithran. Studies on vibration of some rib-stiffened cantilever plates. *Journal of Sound and Vibration*, 57(3):389–402, 1978.

[32] John William Strutt Rayleigh. *The theory of sound: in two volumes. 2*. Macmillan, 1896.

[33] Julian J Rimoli and Raj Kumar Pal. Mechanical response of 3-dimensional tensegrity lattices. *Composites Part B: Engineering*, 115:30–42, 2017.

[34] Walter Ritz. Theorie der transversalschwingungen einer quadratischen platte mit freien rändern. *Annalen der Physik*, 333(4):737–786, 1909.

[35] L Salari-Sharif and L Valdevit. Accurate stiffness measurement of ultralight hollow metallic microlattices by laser vibrometry. *Experimental Mechanics*, 54(8):1491–1495, 2014.

[36] Tobias A Schaedler, Alan J Jacobsen, Anna Torrents, Adam E Sorensen, Jie Lian, Julia R Greer, Lorenzo Valdevit, and Wiliam B Carter. Ultralight metallic microlattices. *Science*, 334(6058):962–965, 2011.

[37] S Tomotika. Lx. the transverse vibration of a square plate clamped at four edges. *The London, Edinburgh, and Dublin Philosophical Magazine and Journal of Science*, 21(142):745–760, 1936.

[38] Francesco Tornabene, Michele Bacciocchi, Nicholas Fantuzzi, and Erasmo Viola. *Laminated Composite Doubly-Curved Shell Structures: Differential Geometry Higher-Order Structural Theories*. Società Editrice Esculapio, 2016.

[39] Lorenzo Valdevit, Scott W Godfrey, Tobias A Schaedler, Alan J Jacobsen, and William B Carter. Compressive strength of hollow microlattices: Experimental characterization, modeling, and optimal design. *Journal of Materials Research*, 28(17):2461–2473, 2013.

[40] Andrea Vigliotti, Vikram S Deshpande, and Damiano Pasini. Non linear constitutive models for lattice materials. *Journal of the Mechanics and Physics of Solids*, 64:44–60, 2014.

[41] Alexander Weinstein and Wei Zang Chien. On the vibrations of a clamped plate under tension. *Quarterly of Applied Mathematics*, 1(1):61–68, 1943.

[42] SX Xu and TS Koko. Finite element analysis and design of actively controlled piezoelectric smart structures. *Finite elements in analysis and design*, 40(3):241–262, 2004.

[43] YF Xu, Da-Ming Chen, and WD Zhu. Damage identification of beam structures using free response shapes obtained by use of a continuously scanning laser doppler vibrometer system. *Mechanical Systems and Signal Processing*, 92:226–247, 2017.

[44] Eiichi Yoshida, Satoshi Murata, Akiya Kamimura, Kohji Tomita, Haruhisa Kurokawa, and Shigeru Kokaji. A self-reconfigurable modular robot: Reconfiguration planning and experiments. *The International Journal of Robotics Research*, 21(10-11):903–915, 2002.

[45] Dana Young. Vibration of rectangular plates by ritz method. *J. appl. Mech.*, 17:448–453, 1950.

[46] Alex J Zelhofer and Dennis M Kochmann. On acoustic wave beaming in two-dimensional structural lattices. *International Journal of Solids and Structures*, 115:248–269, 2017.

[47] Xiaoyu Zheng, Howon Lee, Todd H Weisgraber, Maxim Shusteff, Joshua DeOtte, Eric B Duoss, Joshua D Kuntz, Monika M Biener, Qi Ge, Julie A Jackson, et al. Ultralight, ultrastiff mechanical metamaterials. *Science*, 344(6190):1373–1377, 2014.